Journal of
Biomedical Engineering and Medical Devices

Casolaro and Casolaro, J Biomed Eng Med Devic
2016, 1:2

Research Article Open Access

Stimuli-Responsive Hydrogels Bearing α-amino acid Residues: a Potential Platform for Future Therapies

Mario Casolaro[1*] **and Ilaria Casolaro**[2]

[1]*Department of Biotechnology, Chemistry and Pharmacy, University of Siena, Siena, Italy*

[2]*Psychiatry Resident, University of Siena, Siena, Italy*

[*]**Corresponding author:** Mario Casolaro, Department of Biotechnology, Chemistry and Pharmacy, via Aldo Moro 2, University of Siena, 53100-Siena, Italy, Tel: +390577234388; E-mail: mario.casolaro@unisi.it

Rec date: Mar 26, 2016; **Acc date:** May 20, 2016; **Pub date:** May 28, 2016

Abstract

Vinyl hydrogels bearing α-aminoacid residues have been explored as platforms for the treatment of cancer, glaucoma and mood disorder therapies. Ionic/ionizable groups of the L-valine, L-phenylalanine and L-histidine residues are able to modify the swelling properties of the hydrogel on the basis of their thermodynamic characteristics. Greater basicity constants of functional groups improve a greater loading of the drug and a longer sustained-release pattern. The pH and the temperature affect the swelling of the hydrogel and increase 'on demand' the drug availability. A further stimulus based on alternating magnetic fields can be applied on hydrogels containing embedded magnetic nanoparticles used for site-specific controlled drug delivery. The diffusion process for the *in vitro* release of the drug (cisplatin, doxorubicin, pilocarpine, trazodone, citalopram and paroxetine) from the drug-loaded hydrogels is mainly controlled by the drug-polymer interaction, that in the meanwhile preservs it's bioactivity. The different interaction strength between the drug and the polymer may be a strategy to develop suitable capsules for long-term therapies.

Keywords: Stimuli-responsive hydrogels; Drug release; Protonation thermodynamics

Introduction

A large amount of research work has been performed for the synthesis of new polymers (soluble and cross-linked) in view of their special applications [1-8]. In contrast to most hard materials, the three-dimensional cross-linked networks of water-soluble polymers (hydrogels) may retain a large amount of water within their porous structure and thus they can undergo large deformations. Since hydrogels have structural and compositional similarities compared to the extracellular matrices and their extensive framework for cellular proliferation and survival, they have long attracted considerable attention for various biomedical purposes [9-13]. Although conventional hydrogels show limited changes in the equilibrium swelling with the change of the surrounding environment, polyelectrolyte hydrogels show various unique responses to environmental stimuli including electrically-induced chemomechanical contraction similar to biological responses [14-17]. Furthermore, biological tissues consist of polyelectrolytes, such as charged filamentous proteins, and their properties originate from the polyelectrolyte nature [18,19]. Therefore, polyelectrolyte hydrogels have shown considerable potential as bio-tissue model system to be used for biological experiments and as biomaterials to replace damaged tissues [20]. The swelling of hydrogels can be dependent on various parameters, such as pH, temperature, ionic strength of the surrounding medium and external applied electric and electromagnetic fields. An important group of polyelectrolyte hydrogels is that of N-alkyl acrylamide homopolymers and copolymers with acid/base functional groups of α-aminoacid residues [21-25]; these multiple stimuli-responsive hydrogels have attracted significant research interest because the most pH- and temperature-sensitive dual functional systems have a great importance in biological applications and can well mimic the responsive macromolecules found in nature. In the form of homopolymers or as copolymers with thermosensitive units, like the N-isopropylacrylamide (Nip), the hydrogels may constitute useful materials responding to various external stimuli. Poly(N-isopropylacrylamide) (pNip) has received considerable attention since its lower critical solution temperature (LCST) of 32°C approaches the normal body temperature [23,26-28]. The LCST can be increased or decreased by the incorporation of hydrophilic/charged or hydrophobic comonomers, respectively [22,24,29,30]. Hydrogels can be virtually made from any water-soluble polymer, encopassing a wide range of chemical compositions and bulk physical properties; they can be formulated in a variety of physical forms, including slabs, microparticles, nanoparticles, coatings, and films. As a result, hydrogels are commonly used in the clinical practice and experimental medicine for tissue engineering and regenerative medicine [31], diagnostics [32], separation of biomolecules or cells [33], and barrier materials to regulate biological adhesion [34]. Their porous structure can be easily tuned by controlling the cross-link density in the gel matrix and the affinity of the hydrogels for the aqueous environment in which they are swollen. Their porosity improves loading of drugs into the matrix of the gel and the subsequent drug release at a rate dependent on the diffusion coefficient of the small molecule or macromolecule through the network.

The aim of this paper is to review some of the fundamental properties and the potential biomedical applications of polyelectrolytes hydrogels considered so far to be a convenient platform for future therapies [35-40]. In the recent years, the potential applications of some polyelectrolyte hydrogels as carriers for therapeutic delivery have been explored [5,24] basically for the treatment of cancer [12,41-43], glaucoma [44], and mood disorders [45]. Either new or conventional

metal-based drugs have been considered, as well as drugs used in the clinical practice.

Thermodynamic Characterization of Hydrogels (Basicity Constants, Swelling)

Stimuli-responsive polyelectrolytes, in the free or in the cross-linked gel form, having a vinyl structure and containing convenient functional groups, are usually obtained by radical polymerization of the corresponding monomers in a suitable organic and/or water solvent [5,46]. The monomers may be either commercial or purposely synthesized to improve novel properties of the desired material. Usually, vinyl monomers containing α-aminoacid residues are prepared by the acylation reaction of acryloyl or methacryloyl chloride with the appropriate aminoacid in alkaline solution [5,47]. The reaction must take place slowly at low temperature (-5°C) and in the presence of polymerization inhibitors to prevent side reactions. An external bath of ice and salt is sufficient to keep the temperature low during the dripping of the acryloyl (methacryloyl) chloride to the basic solution of the aminoacid. After neutralization with concentrated hydrochloric acid, the monomer may be crystallized with analytic grade, as shown by potentiometric and spectroscopic (1H-NMR and FT-IR spectra) characterizations. In most cases, white crystals [48] were obtained from water (for acrylic monomers) or from benzene (for methacrylic monomers). They were stable to atmospheric moisture and can be preserved for several months at low temperature. The structure of some synthetic monomers is reported in Table 1.

N-acryloyl-L-valine (Ava)	N-acryloyl-L-phenylalanine (Phe)	N-acryloyl-L-histidine (Hist)	N-methacryloyl-L-histidine (MHist)
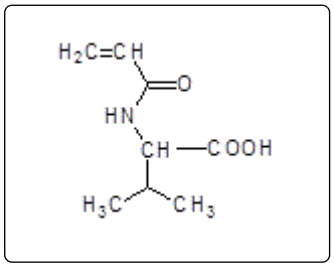	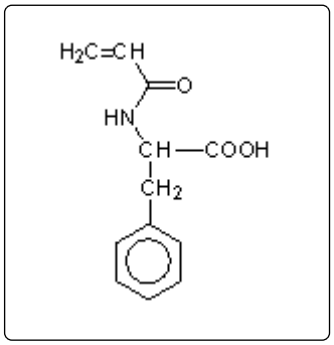	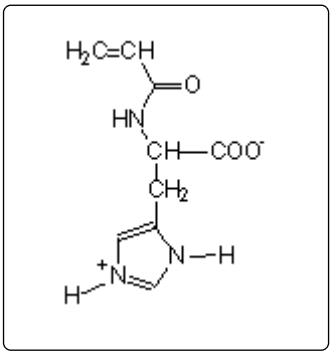	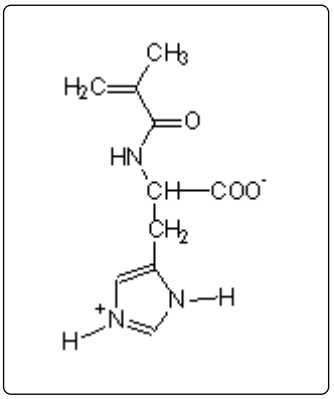

Table 1: Structures of vinyl monomers.

Vinyl polymers, in the linear and soluble form, are generally obtained as homopolymers or as copolymers of the synthetic monomers with the commercial Nip in a variable amount; the reaction takes place in solvents (dioxane, benzene, water) and in the presence of a radical initiator, at 60°C. The potentiometric titration has always shown the content of acid and/or basic groups in the macromolecule to be in line with the feed composition [30,49].

Name of the hydrogel	Type and amount of cross-linking agent (mol%)	Ionic monomer/Nip molar ratio (mol/mol)
Ava-1	EBA (1)	-
Ava-2	EBA (2)	-
Ava-5	EBA (5)	-
Phe-9	EBA (9)	-
Phe-Nip3	EBA (2)	1/1
CP-2	EBA (2)	1/10
Hist-5	EBA (5)	-
Hist-10	EBA (10)	-
CH-1 (Nip-His-1)	EBA (1)	1/12
CH-9 (Nip-His-9)	EBA (9)	1/12
MHist-2 (MH-2)	EBA (2)	-
CMH-2 (Nip-MHis-2)	EBA (2)	1/12
Ava-Nip-Peg258	PEG258 (12)	1/9
Ava-Nip-Peg575	PEG575 (12)	1/9
Phe-Nip-Peg258	PEG258 (12)	1/9

MHist-Nip-Peg258	PEG258 (12)	1/9

Table 2: Composition of the considered hydrogels.

Besides the free polymer analogues, the corresponding hydrogels are formed as insoluble and swellable materials, at room temperature and in the presence of a cross-linking agent, starting by the appropriate monomers dissolved in water and using the ammonium peroxo-disulfate (APS) as a radical initiator. Moreover, free and cross-linked copolymers with different comonomer compositions were obtained together with the Nip. The acid-base titrations of the ionizable group present in the polymer indicated that the comonomer feed ratios reflect the relative comonomer incorporation levels and, in some cases, its random or blocky distribution [50]. The acid/base potentiometric analysis of most of the copolymers suggested a random distribution of charged units along the macromolecule. Gelification of the products was improved with different cross-linking agents, like the N,N'-ethylene-bisacrylamide (EBA) and the poly(ethyleneglycol)diacrylate (PEG-DA) of different molecular weight (Mn 258 and 575). The latter improved more porous materials [51]. In all cases, the polymerization reaction was carried out in water by using a different cross-linking degree. Some hydrogels, incorporating a different amount of $CoFe_2O_4$ magnetic NPs, were obtained by radical copolymerization of the two vinyl monomers: the Nip and the synthetic N-acryloyl-L-phenylalanine in a Nip/Phe molar ratio of 1 [52]. The EBA cross-linking agent was used throughout in a 2 mol% concentration. The hydrogels were prepared in the presence of commercially available magnetic nanoparticles ($CoFe_2O_4$) [53], or embedded with NPs on preformed hydrogels following a synthetic procedure to prepare Fe_3O_4 from Fe(II) and Fe(III) salts in the presence of NH_3 [54,55]. The obtained gel samples, treated with hydrochloric acid solution, collapsed to a small volume; they were obtained in the dry form, as tightly solid, after washing and drying the cutted samples. Unlike normal hydrogels, which show mechanical consistency and transparency, the presence of magnetic NPs makes hydrogels brittle and dark, especially in the dry state. The morphology of the samples is fairly uniform, both in the surface and in the bulk. TEM micrographs of the hydrogel Phe-Nip3 showed that the high density of the nanoparticles is uniformly distributed in the network with a mean diameter of the order of 5 nm [52]. The named hydrogel samples with the comonomers composition is reported in Table 2.

For the thermodynamic characterization of the hydrogels, the protonation-deprotonation equilibrium is the most important chemical phenomenon. Thus, most ionic/ionizable polymers can provide a safe universal platform for administering biologically active compounds which need a more controlled delivery. Since most of pharmacologically active substances contain acidic or basic functional groups which are ionized to varying degree at physiological pH's [56,57], the basicity constants provide an important contribution to understanding structural implications in the mechanism of biological activity. Polyelectrolytes are usually studied in aqueous solution, and their properties are greatly affected by addition of simple salts such as sodium chloride [14,58-60]. The polarity and shape of ionizable polymer chains change considerably with the degree of ionization. Changing the state of the macromolecular chain, for example, by ionizing the carboxyl or the amino group of a polyacid or polybase, respectively, produces electrostatic repulsion along the chain and causes expansion of the originally coiled molecule. The polymer assumes the form of an extended coil when completely ionized and in most cases, coil dimension regularly decreases/increases over the whole range of degree of protonation due to neutralization/protonation of the carboxylate/amino groups and the accompanying electrostatic forces. Hydrophobic groups on polymers may provide further chain contraction, and in some cases the polymer precipitates because the hydrophobic moiety overcomes the hydrophilic quality of the groups being protonated [61]. Macromolecular extension and contraction can be magnified by constructing a three-dimensional polymer network in hydrogels and the feasibility of using such systems as switches for drug delivery devices has been the subject of considerable research. The ionization of the carboxyl acid group onto the polymer, along with the ionic strength, plays a sensitive role in the swelling/deswelling process. Unlike the free aminoacids, showing low basicity constants (logK) for the protonation of the COO^- group, due to the presence of the closer protonated amino group, a greater logK was evaluated for the carboxyl group in the corresponding polymers (Table 3) [14,46,49,61]. On the other hand, the poly(ampholyte) hydrogels, based on vinyl acrylates and methacrylates carrying the L-histidine residues in the side chain, are a special class of polyelectrolytes which contains both positive and negative charges regularly inserted on each monomer unit [7,15,25,62,63]. The imidazole nitrogen of the histidine residue is responsible for most of the buffering capacity of proteins in the physiological range of pH. It is also able of combining with various metal ions and appears to constitute the principal site for metal binding in proteins [64].

Compound	Ionic Strength (mol/L)	$logK_1^{\circ}$ a)	$logK_2^{\circ}$ a)	n1 a)
Mono Ava	0.1	3.47		-
Poly Ava	0.1	4.59		2.26
Gel Ava-2	0.15	4.35		2.07
	0.01	4.84		2.02
Gel Ava-5	0.15	4.44		1.85
	0.01	4.88		2.03
Mono Phe	0.15	3.34		-
Poly Phe	0.15	5.45		-
Gel Phe-9	0.15	4.82		1.1
Gel Phe-Nip3	0.15	4.75		-
Mono Hist	0.15	6.48	-	-
Poly Hist	0.15	7.64	2.3	2.22
Poly(Hist-co-Nip)	0.15	7.11	2.9	1.76
Gel Hist-5	0.15	7.6	2.4	1.96
Gel Hist-10	0.15	7.74	2.9	1.66
Mono MHist	0.15	6.88	-	-
Poly (MHist)	0.15	7.53	2	1.49

Poly(MHist-co-Nip)$_{0.3}$	0.15	7.06	2.5	1.41
Poly(MHist-co-Nip)$_{0.1}$	0.15	6.84	2.8	1.23
Poly(MHist-co-Nip)$_{0.05}$	0.15	6.7	2.8	1.15
Gel MHist-2	0.15	7.66	2.5	1.29

Table 3: Basicitiy constants (logK°) of the monomers and related polymers in the free and in the cross-linked gel forms (25°C). a) logKi=logKi°+(n_i-1)log[(1- α)/ α] (α is the degree of protonation).

As a rule, in the polymeric compounds the logK value was found to be 'apparent', i.e., it depends on the degree of protonation of the whole macromolecule [59,65]. Thus, the polymers showed a polyelectrolyte behaviour either in the free and in the cross-linked gel form. In all cases, the logK was generally found to decrease in a linear manner as the degree of protonation increased, following the modified Henderson-Hasselbalch equation [66]:

$$\log K = \log K^{\circ} + (n-1)\log[(1-\alpha)/\alpha]$$

where α is the degree of protonation of the whole macromolecule and logK° is the basicity constant value, as evaluated at α =0.5. Further, the n value is related to the electrostatic interaction magnitude and to the hydrophilic quality of the polymer; greater n values (n>1) suggest a decreasing logK upon protonation. The presence of Nip units in the copolymeric compounds (free and cross-linked) led to a further decrease of both logK° and polyelectrolyte effect [14,49,60]. The uncharged Nip unit shielded charges along the macromolecule, developing a lower electrostatic effect [65]; this behavior was only attributed to copolymers having a random charge distribution along the polymer. At very low amount of charged units, the logK° approaches the lower value of the corresponding non-macromolecular analogue. Moreover, the protonation data of the free polymer analogues may well support the mechanism of the corresponding hydrogel protonation process. The polyelectrolyte behavior of the charged L-valine and L-phenylalanine residues within the cross-linked polymers was found to be similar to those of the soluble free polymer analogs [44,49]. Figure 1 reveals two characteristic features.

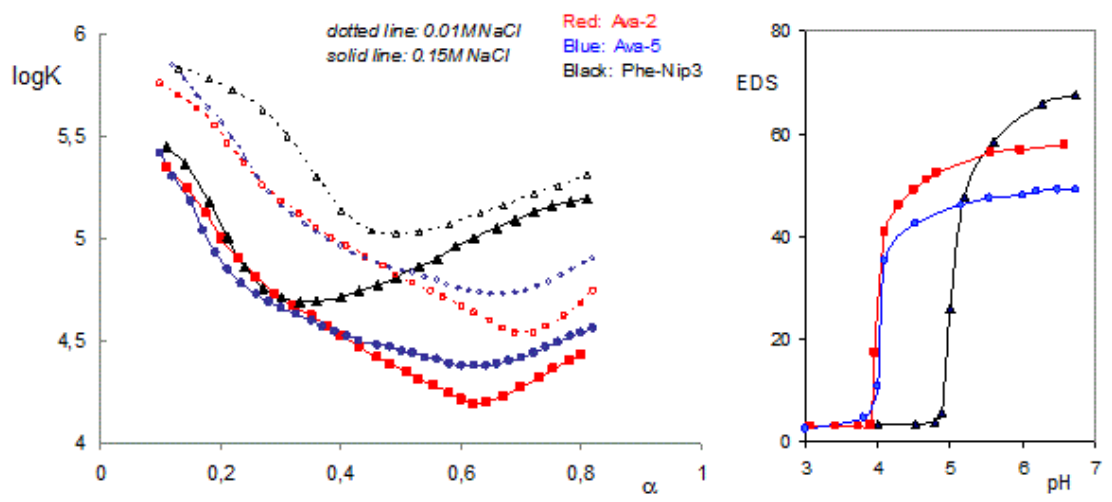

Figure 1: Left: Basicity constants (logK) in relation to the degree of protonation α of the hydrogels Phe-Nip3 (black lines), Ava-2 (red lines) and Ava-5 (blue lines) at 25°C and at two different ionic strengths (solid line: 0.15M NaCl; dotted line: 0.01M NaCl). Right: Equilibrium degree of swelling (EDS) in relation to pH for the hydrogel Phe-Nip3 (black line), Ava-2 (red line), and Ava-5 (blue line) at 25°C and 0.15M NaCl.

At the same ionic strength, the three different hydrogels show a different polyelectrolyte behavior. As the ionic strength becomes lower, the logK value increases. This is a general trend observed in the polyelectrolyte domain, where electrostatic effects are dominant. As regards the copolymeric hydrogel Phe-Nip3, the protonation process led to a decreasing trend of the logK with increasing α up to ~ 0.3 and 0.5 for 0.15 M and 0.01 M NaCl, respectively [45,49,52]. In these low-range of α values the electrostatic effect is predominant and the hydrogel contracts (de-swells) upon protonation of the COO^- groups. Above the critical α values, the electrostatic forces interfere with the hydrophobic ones, due to the presence of isopropyl and phenyl groups located into the hydrogel. This effect, similar to the free polymer analogs, results in a higher logK value upon protonation, due to the abundant exposure of the remaining COO^- groups to incoming protons. The two homopolymers with L-valine residues (Ava-2 and Ava-5), even in the cross-linked form, show a similar polyelectrolyte behavior of the corresponding free polymer [45,52,61]. The lower n value of the corresponding hydrogels may be ascribed to the decreased conformational freedom of the macromolecules because of the slightly cross-linking density. A greater cross-linking degree led to a lower n value. Once again, the decrease of the logK in relation to α is due to charge neutralization; this always lowers the electrostatic effect exerted by the repulsion of the COO^- groups, giving rise to lowering of the magnitude of the macromolecular coil and/or to a decreased hydration of the whole macromolecule. When a critical value of α is exceeded, the forces of electrostatic repulsion of the remaining COO^- are overwhelmed by the forces of hydrophobic nature that stimulate attraction between the isopropyl groups of the side polymer chains [46,60,61]. Naturally, a decreased ionic strength lowers the shielding effect of the COO^- groups and their protonation leads to a higher logK and to an effect of electrostatic repulsion that takes greater degree of

protonation to counteract the hydrophobic effect. The critical value of α then moves to significantly higher values.

The swelling property (equilibrium degree of swelling, EDS) of the hydrogels is strongly dependent on the nature of the α -aminoacid residues and on the degree of cross-linking. The EDS phenomenon observed in Figure 1 may well be related to the logK's behavior. The swelling property of the hydrogels carrying L-valine residues (Ava) is very sensitive to pH changes. It shows a sharp decrease of the EDS in correspondence of a pH value close to the critical degree of protonation of the carboxylate anion [61]. This degree of protonation, corresponding to 0.66, was related to the collapse of the macromolecular coil that forces the isopropyl groups in a close contact, outweighing the repulsive electrostatic interactions of the partially ionized polymer in a more extended and hydrated conformation. At pH>4, the EDS value regularly increases with the increasing charge density of the network. As evaluated by the 'apparent' logK of the hydrogel, the charge density of the COO^- group reaches about 100% in physiological conditions (pH 7.4), while only a value of 34% may be considered at pH 4. It is evident that at pH>4 the EDS increase is greater for the hydrogel Ava-2, due to a lower amount of cross-links in the network. The pH of the phase transition becomes slightly higher at low ionic strength. This is in line with the fact that low ionic strength increases the basicity constant of the carboxylate group, despite its similar polyelectrolyte quality (Table 3). Moreover, the EDS/pH plot of the hydrogel Phe-Nip3 shows that the pH of the collapsing process approaches a value of 5. This greater value is related to hydrophobic interactions that early prevail over the electrostatic repulsion above the critical degree of protonation value of the COO^- groups. The hydrophylic-hydrophobic quality of the functional groups corroborates the phase transitions occurring into the hydrogel. It is worth noting that the pH that triggers the shrinking depends on the logK of the carboxylic group belonging to the α -aminoacid residues. The logK of Phe residues in the linear polymer analogs is always greater than that of the Ava moiety [49,61]. Copolymerization with Nip increases the polyelectrolyte quality of Phe compounds, whereas it decreases that of Ava one; this respectively reflects an increase and a decrease of logK as the degree of protonation increases. Copolymeric hydrogels incorporating a low amount of pH sensitive moieties, like Phe-Nip-Peg258 and Ava-Nip-Peg258 [5,24], collapsed at pH 4.2 and 3.5, respectively [24]. Moreover, the longer segments of Peg575 cross-linker led to higher EDS and lower pH values for the collapsing process. This is likely ascribed to a further low logK of the ionized carboxylic groups that, being more distant from each other, created an environment with a lower electrostatic field. The hydrophilic character of the Peg segments may furtherly enhance the swelling of the network [24].

Drug Delivery and Biomedical Applications

This section includes the study of the controlled release of specific drugs that have been loaded on hydrogels. The drugs are used in clinical practice for various therapies: mood disorders, cancer and eye diseases. Table 4 shows the chemical structure of the drug associated with the value of the basicity constants (logK), useful for understanding the thermodynamic interaction between the drug and the polymer.

Sadness or downswings in mood are normal reactions to life's struggles, setbacks, and disappointments. Many people use the word 'depression' to explain these kinds of feelings, but depression is much more than just sadness. Whatever the symptoms, depression is different from normal sadness in that it engulfs your day-to-day life, interfering with your ability to work, study, eat, sleep, and have fun. Depression is a major risk factor for suicide [67]. In this section we provide some data for the sustained release of amino-ionized antidepressant drugs (citalopram hydrobromide, paroxetine hydrochloride and trazodone hydrochloride) from polyelectrolyte platforms based on anionic hydrogels bearing carboxyl groups of the L-phenylalanine and L-valine residues [44,45,49,52].

Drug	logK
Paroxetine 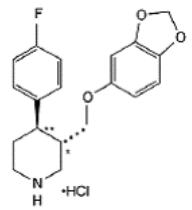	9.52
Citalopram 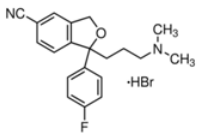	9.42
Trazodone 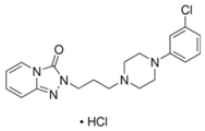	6.89
Doxorubicin 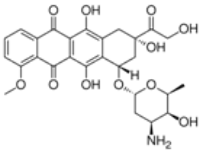	8.3
Pilocarpine 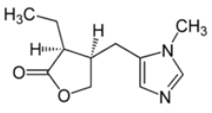	7.2

Table 4: Basicity constants of ionizable drugs used in this study.

There are many types of cancer treatment. The type of treatment required depends on the type of cancer and as it is advanced. Chemotherapy is a type of cancer treatment that uses drugs to kill cancer cells; it works by stopping or slowing the growth of cancer cells, which grow and divide quickly. Chemotherapy not only kills fast-growing cancer cells, but also kills or slows the growth of healthy cells that grow and divide quickly. For this reason, and to avoid damaging collateral problems, the use of polymeric carriers controlling the release of the drug is extremely useful for cancer treatment.

Glaucoma is a group of eye diseases which in most cases produce increased pressure within the eye. This elevated pressure is caused by a

backup of fluid in the eye. Over time, it causes damage to the optic nerve. Glaucoma can be treated with eye drops, pills, laser surgery, traditional surgery or a combination of these methods. The goal of any treatment is to prevent loss of vision, as vision loss from glaucoma is irreversible.

Mood disorders

Mood disorders are a group of disorders considered to be primary disturbances of mood. These include: a) major depressive disorder where a person has at least two weeks of depressed mood or a loss of interest or pleasure in nearly all activities; b) dysthymia, a state of chronic depressed mood, the symptoms of which do not meet the severity of a major depressive episode; c) bipolar disorder, which features one or more episodes of abnormally elevated mood, cognition and energy levels, but may also involve one or more episodes of depression. Depressive illnesses are disorders of the brain, most likely caused by a combination of genetic, biological, environmental, and psychological factors. Depression is a state of low mood and aversion to activity that can affect a person's thoughts, behavior, feelings and sense of well-being. People with depressed mood can feel sad, anxious, empty, hopeless, helpless, worthless, guilty, irritable, ashamed or restless. They may lose interest in activities that were once pleasurable, experience loss of appetite or overeating, have problems concentrating, remembering details or making decisions, and may contemplate, attempt or commit suicide. Insomnia, excessive sleeping, fatigue, aches, pains, digestive problems or reduced energy may also be present. Major depressive disorder is one of the most common mental disorders in the United States. Each year about 6.7% of U.S. adults experience depression. The average age of onset is 32 years old; additionally, 3.3% of adolescents have experienced a seriously debilitating depressive disorder. Women are 70% more likely than men to experience depression during their lifetime, showing a greater proportion of feelings of sadness, worthlessness, and excessive guilt, together with somatic symptoms, such as appetite, sleep disturbances and fatigue accompanied by pain and anxiety. Biological, life cycle, hormonal and psychosocial factors that women experience may be linked to women's higher depression rate. Men often experience depression feeling very tired, irritable, losing interest in once-pleasurable activities and having difficulty sleeping; they are more likely to turn to alcohol or drugs and may become frustrated, discouraged, irritable, angry, and sometimes abusive. Although women have higher rates of suicide ideation and attempts, suicide rate in men is almost three times greater, choosing more effective methods resulting in the higher rate of success [68,69]. Many people with a depressive illness never seek treatment. But the majority, even those with the most severe depression, can get better with treatment. The main medical treatment for depression is antidepressant medication. Antidepressants primarily work on brain chemicals involved in regulating mood called neurotransmitters, especially serotonin and norepinephrine. All antidepressants must be taken for at least 4 to 6 weeks before they have a full effect. The treatment should be continued for at least 6-12 months to prevent relapse. There is a wide range of antidepressant medication available. Some of the most commercial medications used in therapy are in the form of tablets or solutions of various drug concentration. It is essential that the choice of drug should take into account the side effects. Trazodone, a triazolopyridine derivative, was first synthesized in the '60 s as a second-generation antidepressant and still represents a therapeutic option for depressive disorders with or without an anxiety component. It behaves as an antagonist of serotonin type 2 (5-HT2) and alpha1-adrenergic receptors, and as an inhibitor of 5-HT reuptake (serotonin antagonist-reuptake inhibitors, SARI), representing the prototype of this group of drugs. Despite its existence for nearly 40 years, its mechanism of action continues to be the subject of study and research. The main pharmacological property of trazodone is its antagonism of the receptor for serotonin 5-HT2A (1 mg of trazodone will occupy about half of 5HT2A receptors). At higher doses (50 mg), the antagonism also affects alpha1-adrenergic, histamine H1 and alpha2 receptors. Its ability to block SERT (serotonin transporter) is at least 100 times less potent than its ability to block the 5-HT2A receptor. The action on 5-HT2A, alpha1 and H1 receptors is considered the basis for the drug's hypnotic effect at low doses (25-100 mg), while the simultaneous blocking of 5-HT2A and SERT is required for its antidepressant effect, which occurs at higher doses (150-600 mg). The combined action of 5-HT2A antagonism and SERT blocking leads to positive clinical implications in terms of tolerability. In the past, it was assumed that only the 5-HT2A antagonism was sufficient to induce sleep. However, although 10 mg of trazodone are sufficient to saturate almost 100% of 5-HT2A receptors, its hypnotic effect appears only at higher doses, which suggests that the drug also acts on alpha1 and H1 receptors: at these doses, the drug induces and maintains physiological sleep, without causing addiction or residual sedation in the morning, due to its short half-life of 3-6 hours. The adverse effects of trazodone include daytime sleepiness and excessive sedation, headache, dizziness and hypotension. There have been reports of priapism (as in the case of other adrenolytic drugs), with increased libido and extension of nocturnal erections in clinical practice, which is why trazodone is considered effective in the treatment of sexual dysfunction. Trazodone was approved by the FDA for the treatment of major depressive disorder at the end of 1981. Despite the efficacy data emerging from the literature, trazodone has always shown low effectiveness in clinical practice. Nevertheless, thanks to its 5-HT2A receptor antagonism, trazodone has been demonstrated capable of preventing the occurrence of initial and long-term side effects of SSRIs, in particular anxiety, insomnia and sexual dysfunction. Moreover, pharmacological characteristics of the drug clearly suggest the possibility of a synergistic antidepressant action, as well as an increased tolerability, in the case of association between trazodone and SSRI drugs. Despite the interesting hypotheses derived from pharmacodynamic theory, at present there are no studies in the literature to provide the necessary empirical data. Recently, literature data have focused on the use of trazodone in depressive disorders, suggesting the use of sustained-release formulations rather than immediate release ones, which have good potential as hypnotics and the ability to prevent nightmares in major depressive disorder [70-73]. Interest in the drug delivery technology from polyelectrolyte hydrogels may be found for the development of therapeutic systems in the field of mood disorders [45,74,75]. Few results are reported in the literature though depression affects 350 million people around the World, causing 850,000 deaths every year. According to recent estimates, in 2020 it will be the second leading cause of work disability, because of the scientifically proven correlation between job loss, poverty and the disease, with a raise of 0.79% in the suicide rate for each 1% increase in unemployment instalments [67,76]. Yet, with the right diagnosis, drug treatment and social support, remission could be almost always possible. Among the different drugs used in the clinical practice as antidepressant, paroxetine, citalopram and trazodone have been considered for their particular chemical structure. Citalopram is an antidepressant belonging to the class of selective serotonin reuptake inhibitors (SSRIs) [77,78]. It is thought to work by increasing the amount of serotonin, a natural substance in the brain that helps maintaining mental balance. Citalopram is one of the more recent

molecule and, according to numerous studies, the most selective and, therefore, it shows fewer side effects [79]. Differences between newer antidepressants are usually fairly subtle and mostly confined to side effects. Paroxetine shares many of the common adverse effects of SSRIs, including nausea, diarrhea, constipation, dry mouth, somnolence, insomnia, headache, hypomania, blurred vision, loss of appetite, nervousness, paraesthesia, dizziness, asthenia, tremor, sweating and sexual dysfunction [80,81]. Most of these adverse effects are transient and go away with continued treatment. All of these drugs contain a basic nitrogen atom in the molecule and then are subjected to ionization. Their strength of electrostatic interaction with the hydrogel will mainly depend on the logK of the functional groups. A higher value of logK ensures greater stability of the polymer-drug adduct and thus will determine a slower release under physiological conditions. In the present work we proposed to study the sustained release of trazodone from smart hydrogels used as tools for controlled pharmachological release, as well as sustained release of the SSRIs citalopram and paroxetine [45]. The *in vitro* release of the antidepressant from the antidepressant-loaded hydrogels was evaluated at two different pH values (PBS pH 7.4; acetate buffer pH 4.6). Moreover, a mild AMF stimulation (20 kHz and 50 V) was applied to the nanocomposite gel Phe-Nip3 incorporating magnetic ($CoFe_2O_4$) nanoparticles [45,52]. In PBS solution, the release profile showed a different kinetic pattern for the three different drugs. Trazodone was always released faster than citalopram and paroxetine, irrespective of the gel used (Phe-Nip3, Ava-2). Moreover, the release of the drug was much faster with the gel Ava-2. Figure 2 shows the comparative results.

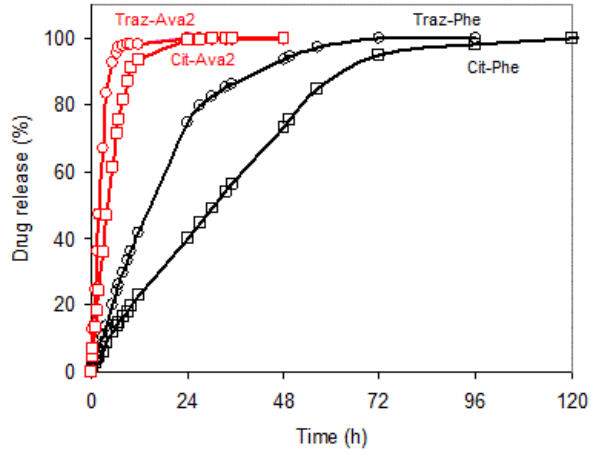

Figure 2: Releasing profiles (%) of citalopram (squares) and trazodone (circles) by the hydrogels Phe-Nip3 (dark lines) and Ava-2 (red lines) at 25°C in PBS (pH 7.40).

The slower release of the citalopram may be related to the greater force of interaction between the drug and the hydrogel. Trazodone, having a smaller basicity constant (logK=6.89) [45,82,83], electrostatically interacts less strongly with the gel and therefore is subject to a faster detachment. This chemical mechanism is also accompanied by a mechanism of diffusion through the gel which may depend on other factors. Among the latter we can include the kinetics of swelling and the possible hydrophobic interactions drug-polymer that can delay the diffusion process. As for the kinetics of swelling, the gel Ava-2 in the ionized form clearly exceeds that of the gel Phe-Nip3. In support of this is the achievement of the plateau in less than 24 hours for Ava-2, while for Phe-Nip3 is required a longer time of over 72 hours. At the end of the releasing process the gel has a full swelling with EDS of 45 and 35, respectively for citalopram and trazodone; the lower value of EDS for the gel containing trazodone is due to the decreased ionization of the carboxyl group for the proton shared with the drug. On the other hand, the different chemical structures of the drugs leave assume a greater affinity of the phenyl groups of citalopram with the phenyl groups of the gel Phe-Nip3. A probable hydrophobic interaction between the phenyl groups delay the release of the drug from the macromolecular network [49]. In any case, the final quantity of the released drug is consistent with the loading data.

To trigger the drug releasing from the drug-loaded hydrogel Phe-Nip3, an alternating magnetic field (AMF) stimulus of low frequency (20 kHz, 50 V) was used. The release profiles of trazodone, citalopram and paroxetine in PBS solution is comparatively shown in Figure 3.

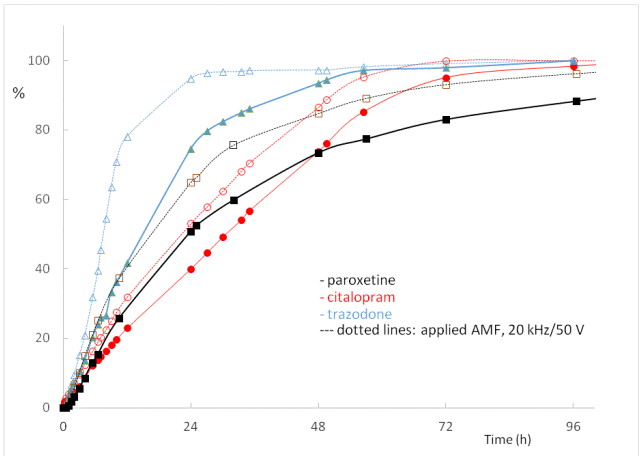

Figure 3: Releasing profiles (%) of paroxetine (dark lines), citalopram (red lines) and trazodone (blue lines) by the hydrogels Phe-Nip3 at 25°C in PBS (pH 7.4) with (dotted lines) and without (solid lines) the AMF (20 kHz, 50 V) application.

In all cases, the release kinetics was increased under the AMF application. Trazodone was released much faster than citalopram and paroxetine, and the complete discharge of the drug from the gel occurred faster than that observed without AMF. During the period of AMF application the temperature remained always constant to 25°C, meaning that all the effects enhancing the diffusion rate of the drug was caused by the oscillation and vibration of the network-embedded $CoFe_2O_4$ magnetic nanoparticles, in a similar manner as for the release of doxorubicin through the doxorubicin-loaded gel Phe-Nip3 [52].

Cancer treatment

Promising ruthenium-based chemotherapeutics are currently under study in clinical trials to fight metastases and colon cancer [84,85]. Moreover, some new drugs based on platinum- and copper-oxicam complexes were recently reported for their anti-cancer activity [42,43]. Among the antitumor agents, cisplatin is commonly used in clinical practice for the treatment of a variety of solid tumors, even though many severe side toxic effects arise [86,87]. Recent strategies aimed at overcoming some drawbacks of cisplatin consist in developing

platforms for chemotherapy that deliver the drug to the local environment of the tumor for extended periods of time [88]. These platforms are based on polyelectrolyte hydrogels carrying functional groups able to form liable complexes with Pt(II)-species [12,41,86,89]. The cisplatin entrapped or complexed in polymeric devices has a reduced systemic toxicity and an increased activity. An example of the strategic device to release cisplatin is based on microparticles; these were obtained with two polymers, poly(acrylic acid) and poly(methyl methacrylate), used as building blocks for their biocompatibility in many cases. Acrylic polymers have exhibited high *in vivo* tolerance in rats after subcutaneous implantation and the carboxylic acid groups can form hydrogen bonds with the glycoprotein coating the mucosal surfaces [90]. To improve these properties and to create more attachment sites for a wide range of therapeutics, some vinyl hydrogels containing α -aminoacid residues have recently been proposed as novel polymeric compounds to get tunable delivery rate of the drug [15,24,25,41,49,62,91,92]. The valine moiety contains, besides the carboxylic group, the amido and the isopropyl groups in a structure closer to that of the Nip. This will render the material pH and temperature-responsive in aqueous solution. The interaction between the Pt(II)-species and the hydrogel allows a chemical-controlled, along with the diffusion-controlled, mechanism. The cisplatin was loaded from the aqueous solution and the release rate, as well as the cytotoxic properties, were studied to find a correlation with the degree of cross-linking. The interaction of the Pt(II)-species with the carboxyl groups led to a charge neutralization of the polymer that improved a collapse of the network. When in the dry form, the Pt(II)-polymer material showed yellowish particles of tightly compact form. The structure of the Pt (II)-hydrogel complex involves a stoichiometry with two closer COO^- groups for each Pt(II)-species. The interaction between the COO^-groups of the closer monomer units and the aminated Pt(II)-species was supported by FT-IR spectra. In the case of hydrogels with L-valine and L-phenylalanine residues we reported the stretching frequencies of the carboxyl and amino group to support the interaction with cisplatin [12,41]. On the other hand, the Pt(II)-species was not able to form stable complex species with copolymers incorporating Nip moieties, because of the great distance and failure in anchoring two COO^-groups of different monomer units. The uncharged and randomly distributed Nip monomeric units showing a shielding effect on the COO^- groups, leads to a lack in the coordination ability. A further feature is the spectral evidence for the presence of the NH3 molecule belonging to the cisplatin that remains linked to the Pt(II)-coordinated species. The 1534 cm^{-1} band, assigned to the N-H bending present in the cisplatin, was already present in the Pt-coordinated hydrogel. This further indicates that the chloride, acting as the leaving group, is responsible for the improvement of the Pt(II)-coordination.

Due to the lower solubility in water (0.25 g/100 g water), the cisplatin was loaded into the hydrogels also in the water/DMSO (98.4:1.6, v/v) mixture [12,89]. In the latter case the DMSO molecule strongly coordinated the cisPt(II)-species allowing reduced or lacking cytotoxic effect upon its release from the hydrogel [12]. The amount of Pt(II)-complex species released from the hydrogels in PBS buffer strongly depends on the initial cisplatin stock solution used for the loading process. The cisplatin solution containing DMSO showed an amount of releasing drug that is more than three times greater with respect to the cisplatin dissolved in water. In both cases, the cumulative release *in vitro* showed to have a biphasic pattern (Figure 4). A burst effect was observed in the first few hours, followed by a sustained release that fitted a near zero-order kinetics.

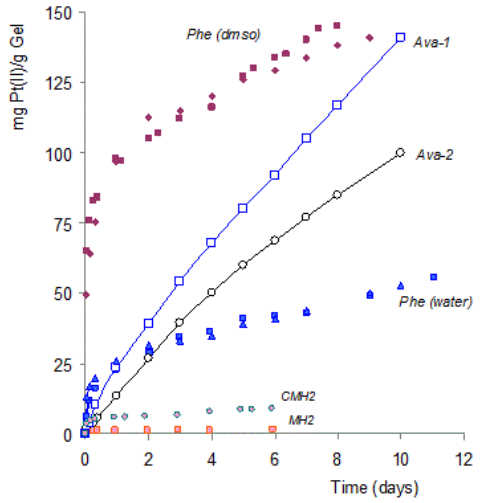

Figure 4: Releasing pattern of Pt(II)-species (Pt/gel, mg/g) from hydrogels Ava-1, Ava-2, CMH2, MH2, and Phe-9 [loaded with cisplatin in water and in water/DMSO solutions], into PBS buffer (pH 7.40, 25°C).

On the other hand, the releasing pattern of the Pt(II)-species from the hydrogel containing the L-valine residues showed an improved linear constant rate for more than one week [41]. This resembles a zero-order release rate which is highly desirable from drug delivery devices [93]. The amount of Pt(II) detected in the downstream PBS buffer solution for the loaded hydrogels containing L-valine residues is also reported in different buffer solutions triggered by the temperature (Figure 5).

This should be a further advantage of the hydrogels to trigger release of the drug in response to the temperature at desired pH values. An increase of temperature to 36°C showed a significantly increased amount of released drug from the hydrogel Ava-2 in PBS solution. For the first four days the release of the Pt(II)-species was linear, as in previous experiments carried out at 25°C. The increase of temperature to 36°C suddenly released Pt(II)-species in the first few hours and then reached a flatter release pattern.

This behavior was correlated to the shrinking phenomenon occurring in temperature-sensitive hydrogels [94]. In the hydrogel Ava-2 the presence of both the functional groups (amido and isopropyl), also present in the classical temperature-sensitive polyNip, together with the Pt(II)-carboxylic coordinated groups, renders this system responsive to temperature also at pH greater than the logK value of the native gel. The strong solvated hydrogel at low temperature, quickly loses the water molecules upon the increasing temperature. This causes the gel to shrink and the diffused Pt(II)-species to split out from the polymeric network. It is noteworthy that the hydrogel Ava-2 shows a larger swelling during the drug release. Moreover, the increasing temperature on the cisplatin-loaded hydrogel is not so effective at lower pH. Unlike the abrupt pH- and temperature-responsivity shown by the native Ava-2 at pH close to 4, the presence of Pt(II)-species anchored to the hydrogel decreases the swelling ability of the network resulting in a lower shrinking phenomenon at pH 4.2 (Figure 5).

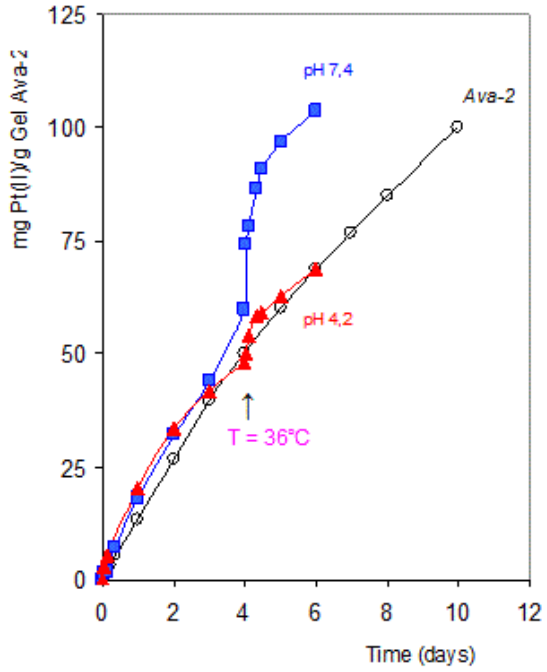

Figure 5: Releasing pattern of Pt(II)-species (Pt/gel, mg/g) from the hydrogel Ava-2 (dark circles) in PBS buffer pH 7.40 at 25°C. Superimposed is the effect of increasing temperature to 36°C for the release of Pt(II)-species at different pH values (blue squares, pH 7.4; red squares, pH 4.2).

Among the considered hydrogels, the Ava one seems to have improved advantages. The use of dry cisplatin-loaded hydrogel sample allows us to know the stoichiometric initial drug source to achieve an extended zero-order release. According to Byrne et al. [93], when a dry hydrogel is immersed in a favorable solvent, the hydrogel transitions in a moving front goes from an unperturbed (glassy) state to a solvated (rubbery) state, with an increase in macromolecular mobility due to chain extension and additional free volume for transport through the gel. The zero-order release arises when a constant rate of solvent front penetration is much smaller than the drug diffusion rate in the swollen gel and this is reported for swelling-controlled hydrogels [95]. In this case, besides the swelling-controlled hydrogel, a further mechanism should be considered. The chemically controlled mechanism, related to the breakage of coordinated Pt(II)-hydrogel bonds, has to be considered together with the diffusion-controlled step. The Pt(II)-species released are subjected to a concentration-dependent diffusion that is related also to the strenght of the complex species with the coordinating groups inside the network. The stepwise binding cleavage and diffusion of the Pt(II)-species from the inner to the external interface of the hydrogel reach a broad range of delivery timescales. Thus, the release rate of the Pt(II)-species is determined by the dissociation strenght of the Pt(II)-gel coordinate bonds. These results suggest a faster release of the Pt(II)-species from the lower cross-linked hydrogel Ava-1. The greater slope (15.0 mg/g per day) of the straightline for Ava-1, with respect to that shown by the Ava-2 (11.7 mg/g per day), is in line with an enhanced diffusion process [41]. This is in line with the above reported data for the comparable cross-linked hydrogels (Phe-9), that showed even lower slope (2.7 mg/g per day) of the near zero-order release phase [12]. The pharmacological efficacy of the Pt(II)-species released from the hydrogels was compared with that of the native cisplatin [5,12,24,41]. Moreover, from an interesting point of view in clinical practice, the synergic effect of cisplatin and other drugs, like temsirolimus, was also considered [41]. The temsirolimus is a rapamycin esther, a machrolid antibiotic used as an immunosuppressor drug in the prevention of transplants rejection [96,97]. This immunosuppressor drug is not cytotoxic by itself, but is able to synergistically increase the cytotoxicity of cisplatin. The cytotoxic effect of the native cisplatin was compared to the cytotoxic effect of the Pt(II)-species released from the loaded hydrogels by using the melanoma cells Me665/2/21. The *in vitro* experiments were carried out at concentrations close to the plasma one (1 μg/mL, corresponding to 0.67 μg/mL or 3.3 μM of Pt) found in patients treated with cisplatin for solid tumors [12,41]. In the same experiments, cells were also treated with 30 μg/mL of the hydrogel Phe-9 (containing 8.7 μg/mL or 45 μM of Pt loaded from water); with the hydrogel containing cisplatin loaded from water, which is slower in terms of cisplatin release, melanoma cells received a dose of Pt(II) comparable to that of native cisplatin (0.51 μg/mL or 2.6 μM, released within the first 3 h, see Figure 4). As shown in Table 5, the cisplatin released from the cisplatin-loaded (from water) hydrogel, similar to the native cisplatin, induced a remarkable apoptotic cell death, as evaluated by cell loss, cell detachment from the monolayer, and increased activity of caspase-3/-7, the latter being a well-known hallmark of apoptosis [12].

Sample	Total cell number (× 10^{-6})	% detached/total cells
Control	12.04 ± 0.68	ND
Cisplatin	3.02 ± 0.44	80.8 ± 1.2
Hydrogel-cisplatin (in water)	3.00 ± 0.38	77.0 ± 4.9
Hydrogel-cisplatin (in water:DMSO)	11.22 ± 0.44	ND

Table 5: Me665/2/21 melanoma cells (1.5×10^6) were treated for 72 h with cisplatin (1 μg/mL) or with cisplatin-loaded Phe-9 hydrogels (30 μg/mL, both). The percentages of detached cells on total cells in control (untreated) and in hydrogel-cisplatin (in water:DMSO) samples were minor, ranging from 2 to 5%.

On the contrary, no effect on cell growth and viability was obtained by the same hydrogel Phe-9 loaded with cisplatin from a water/DMSO mixture, although it releases a higher amount of Pt(II)-species. In the latter case, the loss of activity of the Pt(II)-species released from the

hydrogel may be likely attributed to its exclusion into cells because of the charged Pt(II)-complex species anchoring sterically hindered DMSO molecules. Alternatively, the presence of the DMSO molecule in the Pt(II)-complex species could suppress the intercalation between the two DNA strands [98]. Solvolysis reactions of cisplatin in DMSO might be expected to form primarily monofunctional DNA adduct [99]. It is worth that different Pt(II)-species are released from the same hydrogel Phe-9; unlike the Pt(II)-species released from loaded Phe-9 in water, the adduct containing a DMSO molecule has reduced ability to bind double-stranded DNA and therefore, has potentially reduced toxicity [98]. The electrospray MS spectra, as well as the FT-IR spectra, confirmed the composition and the structure of the Pt(II)-DMSO adduct [12]; a prevailing peak at m/z=343 was consistent with the Pt(NH3)2Cl(DMSO) species, and two strong S=O stretching bands at 1028 cm^{-1} and 1124 cm^{-1} clarified the presence of the DMSO molecule. Unlike the cisplatin solution (in water), both mother (in water/DMSO) and sample Pt(II)-species released from the hydrogel showed the presence of a DMSO molecule linked to Pt(II), because of the replacement of a chloride leaving group. This leads to the hypothesis that, once linked, the DMSO molecule remains stably anchored. Thus, the affinity of Pt(II) for sulfur donor ligands makes DMSO unsuitable for use in biological studies of the mechanism of action of platinum antitumor drugs and the results of biologically related experiments employing mixture of solvents containing this molecule must be strongly discouraged. On the other hand, the use of a different solvent, like DMF, does not cause biological problems. This is the case of experimented synergic effect of cisplatin with temsirolimus, the latter loaded on the hydrogel that was swollen in DMF, due to its insolubility in water. Temsirolimus, a rapamycin analog acting through mTOR inhibition, is an approved immunosuppressive agent and it is under investigation as a potential anticancer drug, when combined with other cytotoxic drugs [96,100]. Used in a wide range of concentrations (1-1000 nM) on Me665/2/21 melanoma cells, temsirolimus alone exerts a moderate inhibition of proliferation with no sign of cell death. On the contrary, in the combined treatment using both, the native cisplatin and the temsirolimus, the latter increases cisplatin cytotoxicity, acting through a moderate synergy (Figure 6).

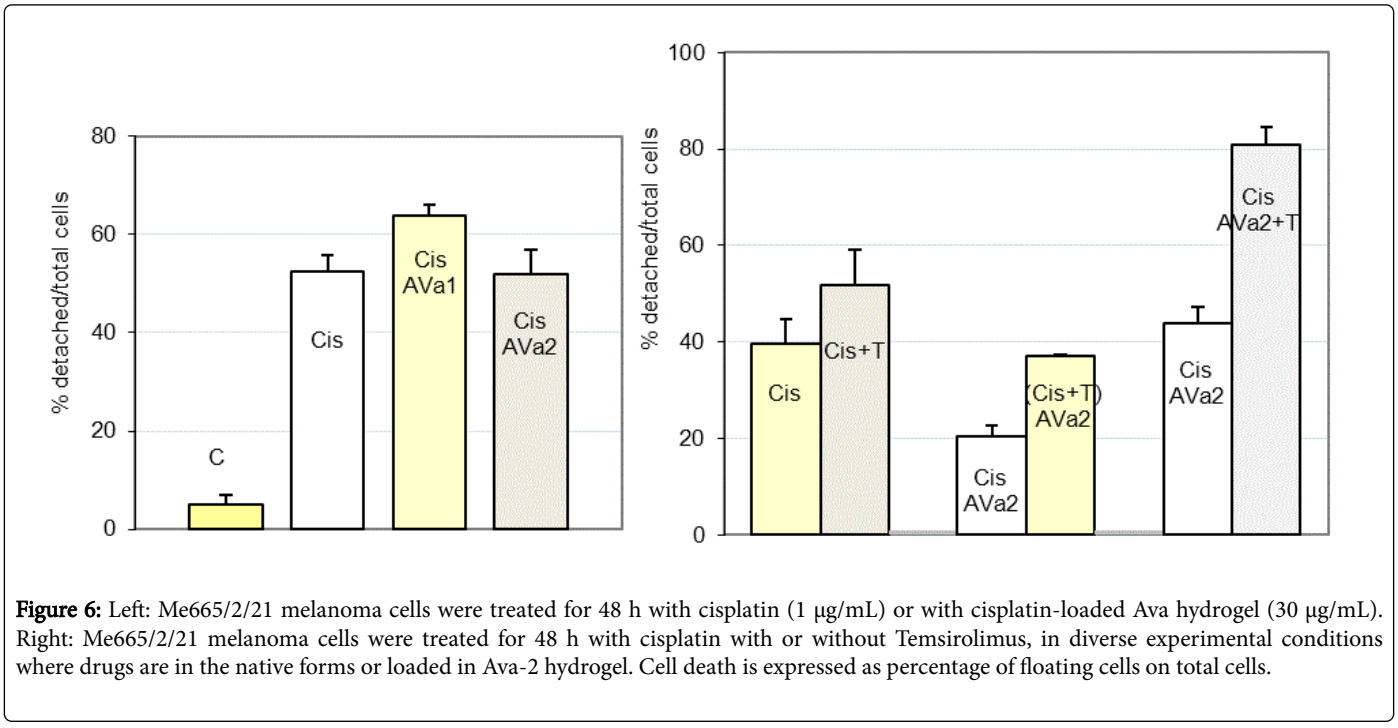

Figure 6: Left: Me665/2/21 melanoma cells were treated for 48 h with cisplatin (1 μg/mL) or with cisplatin-loaded Ava hydrogel (30 μg/mL). Right: Me665/2/21 melanoma cells were treated for 48 h with cisplatin with or without Temsirolimus, in diverse experimental conditions where drugs are in the native forms or loaded in Ava-2 hydrogel. Cell death is expressed as percentage of floating cells on total cells.

When melanoma cells are treated with cisplatin/temsirolimus-loaded Ava-2 hydrogel, the synergic effect is much higher, the contribution of temsirolimus almost doubling the cytotoxic response with respect to the hydrogel loaded with cisplatin alone [41]. It should be noted that, in these experiments, both cisplatin and temsirolimus have been loaded in DMF; in such conditions the release of cisplatin is slower and, consequently, the cytotoxic response is lower. The synergistic cytotoxic response is also remarkable when the native temsirolimus is combined with cisplatin-loaded Ava-2 hydrogel. The extent of apoptotic cell death has been confirmed by Western blot analysis of the caspase-dependent proteolysis of the nuclear enzyme poly(ADP-ribose) polymerase (PARP). PARP cleavage is a hallmark of apoptosis and the ratio between the cleaved moiety and the total protein (full length+fragment) strictly mirrors the extent of both cell death and activation of caspase-3/-7 [41].

As a matter of fact, different drugs may be incorporated into the gel matrix if they are able to ionically interact with the ionized functional groups of the hydrogel. The different strength of the linked drug ensures a different release rate from the hydrogel. This is the case of some ionic/ionizable organic drugs (doxorubicin, pilocarpine, citalopram, paroxetine, trazodone) loaded on the vinyl hydrogels containing α-aminoacid-residues [44,45,52]. Doxorubicin is an antineoplastic chemotherapy drug, one of the most effective anticancer drugs currently known, that is commonly used against breast cancer [101]. Doxorubicin is classified as an 'anthracycline antiobiotic', thus is made from natural products obtained by species of the soil fungus Streptomyces. These drugs act during multiple phases of the cell cycle and are considered cell-cycle specific. However, its clinical use is restricted by dose-dependent toxicity (myelosuppression and cardiotoxicity). Nanotechnology is a promising alternative to overcome these limitations in cancer therapy as it has been shown to reduce the

systemic side-effects and increase the therapeutic effectiveness of drugs [52,102-107]. Some preliminary results for the sustained release of doxorubicin from composite polyelectrolyte hydrogels, a long-term platform-based delivery systems embedded with magnetic nanoparticles [52] are reported as follows. The amount of the released drug can be controlled by fine-tuning the doxorubicin loaded-hydrogel and by external triggers such as temperature and external applied alternating magnetic field (AMF). The *in vitro* doxorubicin release from hydrogels was carried out in PBS at pH 7.4 and 25°C, with and without AMF application. In some cases, the temperature was increased to 37°C in order to evaluate the response of a possible temperature trigger of the temperature-sensitive hydrogels. Furthermore, in this study 'infinite sink conditions' were simulated [108]. Hence, a pre-weighed amount of DOXO-loaded hydrogel in a Strainer cell was suspended in 3 mL and/or 50 mL of the release medium, while the medium was regularly replaced every 24 hours. Figure 7 shows the comparison of the cumulative DOXO release profiles from hydrogel Phe-Nip3 loaded with different amounts of the drug (26 wt% and 48 wt%). The DOXO release profile from gel Ava-2 with 56 wt% loading is also shown for comparison.

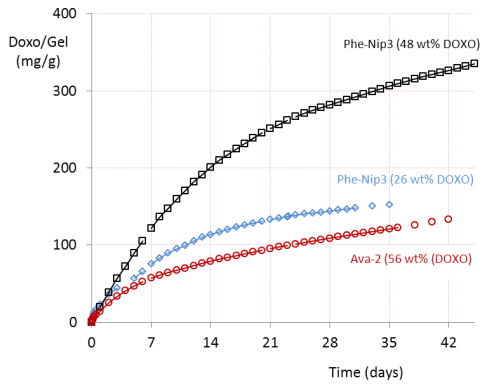

Figure 7: Cumulative release of DOXO (mg/g) from different DOXO-loaded hydrogels: Phe-Nip3, 48 wt% loading (dark); 26 wt% loading (blue); and Ava-2, 56 wt% loading (red). Release experiments were performed in PBS, pH 7.4 at 25°C.

It is evident that, for Phe-Nip-based hydrogels, increased drug loading causes an increased drug release at fixed time intervals. Importantly, electrostatic DOXO-hydrogel interactions play a key role in controlling the amount of free drug available for therapeutic purposes. This is corroborated by the DOXO release profile from hydrogel Ava-2, loaded with a considerably higher quantity of DOXO, compared to hydrogel Phe-Nip3. DOXO is a positively charged molecule with a basicity constant logK of 8.3 [109-111]. It can therefore participate in electrostatic interactions with the ionized carboxyl groups of the hydrogel at pH 7.40.

Complexation takes place with the expected 1:1 stoichiometry. The intensity of this drug-polymer interaction increases as the logK of the COOH moiety of the gel-forming polymer increases. Hydrogel Ava-2 mainly consists of polymer chains of acrylic units with residues of L-valine, slightly cross-linked with EBA. Furthermore, logK values for the COOH groups are higher for the L-valine units, especially at low degrees of protonation and at low ionic strength [15,49,111]. This suggests that hydrogel Ava-2 may form electrostatically more stable complex species with the DOXO molecule [102]. To trigger DOXO release from the hydrogels, two different forms of trigger were used: a temperature stimulus and an AMF stimulus of low frequencies. Figure 8 shows the release profiles from the DOXO-loaded Phe-Nip3 hydrogel (26 wt% DOXO) (panel A), and from the DOXO-loaded Ava-2 hydrogel (56 wt% DOXO (Panel B), in PBS [52].

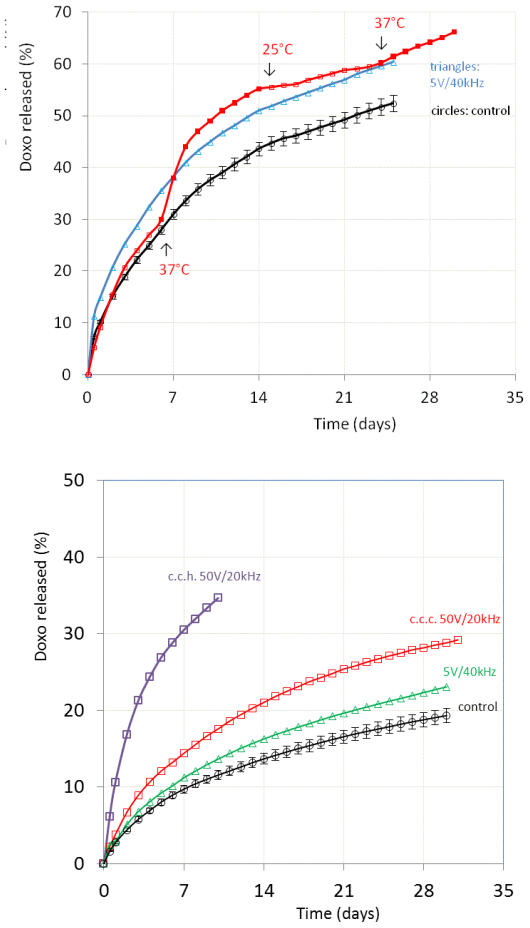

Figure 8: Above: Cumulative DOXO release (%) from DOXO-loaded hydrogel Phe-Nip3, in PBS pH 7.40 at 25°C: under AMF stimulation (40 kHz and 5 V, blue triangles); control (25°C, black circles); effect of the 37°C temperature (red filled squares). Below: Cumulative doxorubicin release (%) from DOXO-loaded hydrogel Ava-2 under different AMF stimulation (PBS pH 7.40 at 25°C): control experiment (black circles) stimulated by 40 kHz and 5 V (green triangles); stimulated by 20 kHz and 50 V with cell copper condenser (c.c.c., red squares); stimulated by 20 kHz and 50 V with copper coil honeycomb (c.c.h., violet squares).

A two-phase release process can be seen when incubated at 25°C. An initial burst-like release is followed by a stable diffusion-controlled release profile. This may be attributed to the initial gel swelling from the dry state. Once hydrated, the hydrogel does not undergo large

changes in swelling as the complexed DOXO molecules prevent fast ionization of the carboxyl groups. The low swelling of the hydrogel, even at longer times, follows the slow kinetics of release of the complexed drug. When temperature increases from 25°C to 37°C, a higher release rate is observed (Figure 8). This enhancement in release rate may be attributed to the collapsing process of the hydrogel, being temperature-sensitive due to the presence of the Nip units.

It is worth-noting that the effect of temperature on hydrogel collapse is pronounced in this case, in contrast to the native hydrogel [52]. This is due to the fact that only a limited number of carboxyl groups are in the uncomplexed state, because of the presence of the complexed DOXO (about 30%). The latter, by partially neutralizing the polymer system, induces a lowering of the LCST. The process of the hydrogel collapse is exhausted in a few days, as evidenced by the subsequent decrease of DOXO released during a week. At 25°C, the release mode restores to a slow profile, becoming comparable to that of the control, for more than a week. In the next cycle of temperature rise from 25°C to 37°C, and after 24 days, the enhancement in release rate is much more limited. In this situation, since the release of DOXO has reached the double value (60%), the shrinking process stops and the hydrogel undergoes changes only due to temperature, similar to the native gel. When the second AMF trigger was applied, the rate of DOXO release was enhanced for extended time. Panel A of Figure 8 shows that DOXO release is significantly accelerated under an applied AMF of low frequency (40 kHz). Exposure of nanocomposite systems to high magnetic fields usually causes a temperature rise in the surrounding environment [112-115]. Therefore, we limited our AMF stimulation to mild conditions in order to avoid heat shock responses [116]. During the application of AMF for the entire duration of the release curve, no temperature increase was observed in the release media (PBS maintained at 25°C). Despite this, the release curve is systematically higher than the control. This increase yields a release profile that is almost identical to that described above, due to temperature increase. An undetected temperature increase inside the hydrogel may be due to the presence of magnetic NPs, stimulated by the applied AMF. This can lead to enhancement of the diffusion rate of the loaded DOXO. Moreover, the energy induced by AMF can cause oscillation or vibration of the network-embedded $CoFe_2O_4$ magnetic nanoparticles [117]. This in turn may cause twisting and/or displacement of the polymeric chains, resulting in an enhancement of the diffusion process. It is believed that the magnetically-induced deformation of the hydrogel, as a result of the oscillation or vibration of the embedded magnetic nanoparticles, is elastic. This elastic deformation ensures a long-term, reliable controlled release of the drug. This permeability control mechanism has also been addressed by other researchers [118-120]. In a similar manner we proceeded to evaluate the long-term release of DOXO from DOXO-loaded hydrogel Ava-2 [52]. The Panel B of Figure 8 summarizes the cumulative DOXO release (%) under different AMF conditions and, even at the same AMF conditions, with different stimulation systems (a cell copper condenser, c.c.c., and a copper coil honeycomb, c.c.h.). Control experiments for each release curve are also shown under appropriate stimulation of AMF. These parallel experiments were done with precisely weighed amounts of hydrogel samples in the same volume of the releasing PBS medium. The release of DOXO from DOXO-loaded hydrogel Ava-2 is enhanced with the application of the same AMF stimulation (40 kHz and 5 V), although to a less extent compared to similar experiment with the Phe-Nip3 hydrogel. This may be ascribed to the lower amount of free DOXO in equilibrium with the strongly hydrogel-complexed DOXO. The magnetic stimulation produces a vibrational state of the polymer network by increasing the diffusion of the drug. Increase in the applied voltage (50 V) and decrease in the frequency (20 kHz) enhance DOXO release. The use of the honeycomb copper coil strongly improves DOXO release kinetics compared to the cell copper condenser. The curves related to the experiment with the generator AG 1006 and with the honeycomb copper coil confirm the greater significance of the magnetic field effects compared to those of the electric field exerted by the cell capacitor. In the first case mechanical stimulation of the magnetic NPs occurs throughout the whole sample mass. This is due to the vibrationally-induced effect with consequent increase of the temperature (about 3°C) of the bathing medium. In the second case, the enhanced DOXO release compared to the control curve (without stimulation) can be attributed only to small currents induced on the surface of the hydrogel sample without affecting the hydrogel inner volume. Indeed, the effects of low and medium frequency electric fields on temperature are limited on the surfaces of the exposed bodies. In the absence of any external stimulus, as well as under the AMF application, the DOXO release profiles for both hydrogels appear to obey the empirical Peppas's power law expression:

$$M_t/M^{\circ}=kt^n$$

where M_t and M° are the cumulative drug releases at time t and infinite time, respectively; k is the rate constant relative to the properties of the matrix and the drug, and the n value is the diffusion exponent characteristic of the release mechanism [121,122]. In the case of pure Fickian release, the n has a limiting value of 0.50 from slabs, whereas values of $0.5<n<1$ indicate a non-Fickian (anomalous) diffusion mechanism. The results of our analysis, conducted on the hydrogel systems, show that for the initial time of release (1 week) the diffusion exponent n for both hydrogels is between 0.58 and 0.91, in the presence and in absence of AMF [52]. The analysis for the successive time period (late release) shows that the n value is less than 0.5 in all cases. Thus, unlike the initial anomalous diffusion mechanism most likely due to the swelling of the dry sample, the release of the DOXO follows a Fickian diffusion mechanism for the period >8 days. These results confirm that the main release mechanism is diffusion, as expected considering the electrostatic hydrogel-DOXO interactions. Furthermore, it is interesting to note that the value of k, though different for the two types of hydrogels, significantly increases with the application of an external stimulus (AMF). This observation may be related to the greater permeability and mobility inside the hydrogel and favoured Fickian release of DOXO inside the network [111,123,124].

Experiments were performed on HeLa cells to compare the cytotoxic effects between native DOXO and DOXO released from the loaded hydrogel Phe-Nip3 [52]. The selected concentration for native DOXO was 2 mM, which was able to induce approximately 50% cell death in our experimental conditions. In an initial set of experiments, HeLa cells were treated with different amounts of DOXO-loaded hydrogel, ranging from 90 to 740 μg. As shown in Figure 9 (Panel A), similarly to the native drug, doxorubicin released from the gel induced a remarkable extent of cell death, as demonstrated by the high percentage of injured cells detached from the monolayer.

As expected, the extent of cell death has a good positive correlation with the DOXO-loaded hydrogel amounts. Similarly to the native drug, DOXO released from the gel stimulates apoptosis in HeLa cells, as demonstrated by two hallmarks of this cell death mode (Figure 9, Panel B): the notable increase of caspase 3/7 activity, and the caspase-dependent proteolysis of PARP protein. The decrease of the full-length

protein, along with the concomitant appearance of the cleavage product, strictly mirrors the extent of apoptosis and, as expected, matches with the levels of cell detachment and caspase -3/-7 activity.

Glaucoma treatment

Pilocarpine is a water-soluble drug widely used in the glaucoma therapy. Since the molecule contains an imidazole ionizable group, the drug may interact with the carboxylate group of the polymer and be subsequently released from the hydrogel [125,126]. The latter may have a useful application as ophthalmic inserts, like the Ocusert-pilocarpine device, due to its valuable properties: non-toxic effect and good optical transmission in the swollen state [44,127-131]. The inserts will increase the contact time between the preparation and the conjunctival tissue, to ensure a sustained release suited to systemic treatment. Compared with the other polymeric ophthalmic devices, the reported hydrogel platforms may have improved advantages as phase transition systems. Changes in external stimuli, like temperature, may trigger the release of the complexed drug, enhancing its bioavailability.

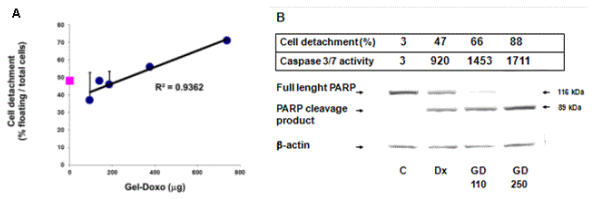

Figure 9: Panel A: HeLa cells were exposed for 18 h to 2 mM native doxorubicin (pink square) or to different amounts of DOXO-loaded Phe-Nip3 hydrogel (blue circles). Cell injury was evaluated as percentage of floating cells on total cells. For native doxorubicin, results are presented as mean ± S.E. of four independent experiments. For DOXO-loaded hydrogel, each point of the plot represents the mean value (± S.E.) of two to four very similar amounts of the sample used in several independent experiments. Panel B: HeLa cells were exposed for 24 h to 2 mM native doxorubicin (Dx) or two amounts of DOXO-loaded hydrogel (GD). Apoptotic cell death was assessed as cell detachment (% of floating cells on total cells), as caspase 3/7 activity (Arbitrary Units of Fluorescence (AUFs)/min/mg protein), and as PARP proteolytic cleavage evaluated in Western blot. β-actin was also revealed and used as loading control. A typical experiment out of three is shown. C=Untreated, control cells.

Pilocarpine reduces pressure in the eye by increasing the amount of fluid that can drain from the eye. Recently, polymeric systems are developing to find a suitable carrier for the ocular drug therapy of most glaucoma patients and to increase the efficacy and the bioavailability of the drug [128,129,132]. Pilocarpine, as a natural parasympathomimetic alkaloid, is an imidazole derivative exhibiting pharmacological activity [125]. The drug has been used in the treatment of chronic open-angle glaucoma and acute angle-closure glaucoma for over 100 years. Among other things, in ophthalmology pilocarpine is also used to reduce the possibility of glare at night from lights if the patient underwent implantation of phakic intraocular lenses; the use of pilocarpine would reduce the size of the pupils, relieving these symptoms. The most common concentration for this use is pilocarpine 1%, the weakest concentration. Since the drug has been widely used topically in the eye, because of its good water solubility, it suffers from the low ocular bioavailability because of its low lipophilicity and the short residence time of aqueous solution in the eye. Pilocarpine is usually administered in the eye by drops of 3 wt % solution. It comes also in eye gel, and in a controlled release system (Ocusert Pilo) [127]. Several papers, based on hydrogels as a platform for new ocular drug delivery, appeared in the literature [44,128,129,132,133]. More recently, the interesting evaluation for the controlled ocular delivery of pilocarpine and its subsequent pupillary constriction of fast forming hydrogels containing thiol groups was reported [132]. On the other hand, the hydrogels based on α - aminoacid residues included anionic and zwitterionic compounds, for electrostatic purposes. Besides the three carboxylic acid materials (based on L-valine), two more compounds of different zwitterionic charge density (containing the L-histidine residues) were taken into consideration [15,44,62]. During the loading process, a reduced size of the swollen Ava hydrogels was revealed. This was attributed to the partial charge neutralization due to electrostatic interactions between the negative ionized groups of the hydrogel and the positively ionized nitrogen of the pilocarpine, being in the hydrochloride form. A deswelling effect of the Ava-2, previously swollen in deionized water, upon the addition of pilocarpine in the form of a stock solution and as a solid dissolving in situ was shown to occur. The initial sharper decrease of the EDS in relation to the wt% of pilocarpine added may be simply ascribed to the ionic interaction of the pilocarpine hydrochloride and the negatively ionized gel [44]. This interaction is not so strong because of the conceptual low stability of the forming complex species between the COO^- of the gel and the protonated pilocarpine molecule. An higher amount of pilocarpine is necessary to reach a stoichiometric break-point, that is theoretically close to a pilocarpine concentration of 0.02 wt%; the fact that, for the end-point, a 5-10 fold excess of pilocarpine is required, is consistent with a low equilibrium constant, that is rather small and products are not quantitatively formed as the drug is added. This hypothesis was also supported by FT-IR spectra of the gel Ava-2 in the ionized form and its adduct with protonated pilocarpine. The small shift of characteristic bands belonging to pilocarpine and the C=O stretching of the gel were indicative of the low interaction. Overall, the pilocarpine is loaded into the gel and its release becomes easier for the low electrostatic interaction. The optical transmission (OT) of the pilocarpine-loaded Ava hydrogels in the swollen state was measured at 480 nm in a 10-mm quartz cuvette, filled with PBS. It was found to be linearly dependent on the cross-link density. On the other hand, the lower swelling of the hydrogels at lower pH values results in a greater opacity. Among the three hydrogels, the Ava-1 showed the best performance with 98% OT (in PBS buffer, pH 7.40), while the other two hydrogels Ava-2 and Ava-5 revealed, respectively, 96% and 90% of OT [44]. In order to load the ocular drug into the network, the swollen hydrogel was soaked in a water solution (3 wt%) of pilocarpine hydrochloride and was kept in this solution for one week. Once loaded, the hydrogels were filtered, washed with distilled water, and finally dried to a constant weight. In all cases, the hydrogel samples showed a relevant weight increase. This increase was also related to the EDS of the particular hydrogel. Higher its EDS, greater results the amount of pilocarpine entrapped into the hydrogel. The release of pilocarpine was monitored in PBS buffer (pH 7.40) by measuring the absorbance at 216 nm of sample solutions taken at intervals. A calibration procedure was previously performed to compare and to evaluate the amount of pilocarpine. The released quantity of drug (mg) per unit weight (g) of dry pilocarpine-loaded gel was summarized for all the hydrogels investigated during the time of a week in Figure 10 [44].

The results clearly show two basic points. First, a burst effect, predominantly due to the physically entrapped pilocarpine, is present in all cases; second, the amount of released pilocarpine is different as different is the nature of the hydrogel [44]. The zwitterionic hydrogel CH-1 showed, after the initial burst effect, a sustained release pattern around 400 mg pilocarpine/g of dry gel. A greater release, around 600 mg/g and more was shown by the hydrogel of the Ava series [44]. The electrostatic effect further contributes to keep the drug more strongly bound inside the network. Thus, the different releasing pattern may be ascribed to the different electrostatic interaction between the pilocarpine and the ionized groups into the network. Pilocarpine is an etherocyclic imidazole derivative having a logK of 7.2 [126,134]; at physiological pH (PBS, pH 7.40) its molecule is mostly in the neutral or positively ionized form.

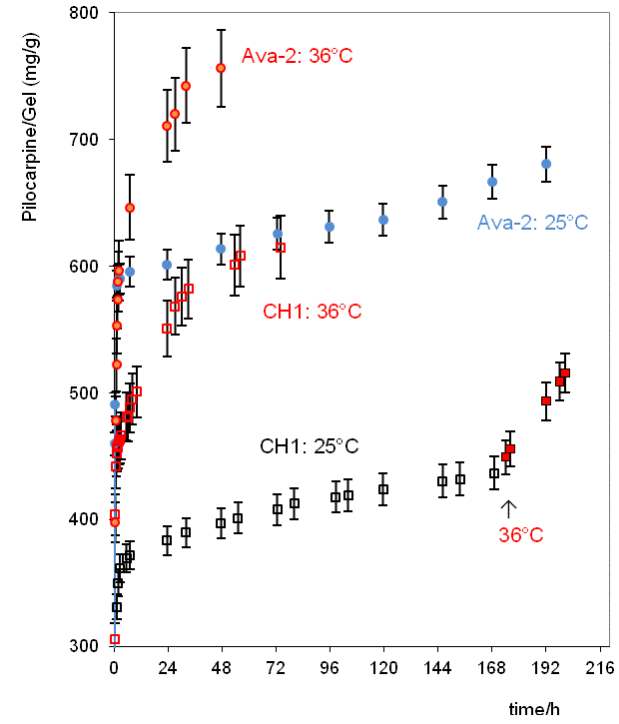

Figure 10: Releasing pattern in PBS (pH 7.40) of pilocarpine (mg/g of gel) from the hydrogels Ava-2 (blue circles at 25°C, and red circles at 36°C) and CH-1 (dark squares at 25°C with pulse of temperature to 36°C, and red squares to 36°C).

As the pilocarpine comes inside the zwitterionic hydrogel, its positively ionized molecule displays electrostatic repulsions with the positively ionized imidazole residues of the gel with Hist, despite the presence of negative carboxylate charges. This latter, having a low logK, weakly interacts with the protonated drug [62]. As the number of charges decreased and the swelling of the hydrogel CH-1 increased, the loading of the pilocarpine was enhanced. Furthermore, in this case a slow sustained release was improved for a week. This behavior was already found for the release of the ferulic acid from the zwitterionic hydrogels [15]. As a matter of fact, the presence of only negative charges, due to carboxylate anions of greater logK values, in the Ava hydrogels, clearly showed the effect of the electrostatic interactions. In all the Ava hydrogels series, the amount of incorporated pilocarpine was almost the same, even the relative EDS value is different, and became greater with respect to the Hist hydrogels. The gel Ava-2 showed a sustained release of pilocarpine for several days [44]. The effect of temperature was also evaluated for the two hydrogels: CH-1 and Ava-2. The releasing profile of pilocarpine at 25°C and 36°C in the same PBS solution is compared (Figure 10). It is noteworthy that the increased temperature displays an increased amount of pilocarpine released. For the hydrogel CH-1, the sustained release of pilocarpine at 25°C, monitored for a week, notably increased for more than one day as the temperature increased to 36°C. At the same temperature of 36°C, the amount of pilocarpine released from the gel CH-1 was higher, within the three experimental days, reaching almost the quantity released from the gel Ava-2. The effect of temperature improved the same behavior for the gel Ava-2, because the releasing profile showed either a greater slope and a greater amount of pilocarpine released within two days at 36°C. This behavior was correlated to the shrinking phenomenon occurring in temperature-sensitive hydrogels [27,135,136]. In the gel CH-1, the presence of the greater Nip content displayed a lower solvation at increased temperature. This caused the gel to shrink and the pilocarpine molecules were gradually splitted out from the polymeric network. Likewise, the gel Ava-2 showed the same behavior, because of its temperature-responsiveness [44].

For the evaluation of the Ava hydrogels cytotoxicity, immortalised mouse fibroblasts NIH3T3 were chosen [44]. Not confluent adhered cells were incubated with 10 mg of each swollen sample, both in the native and loaded with pilocarpine forms. Samples were analysed after 24 hours of incubation and the results showed that all the tested samples were not cytotoxic for the mouse fibroblast 3T3 cells. In particular, the percentage of viable cells in contact with the native samples (Ava-1, Ava-2, and Ava-5) and with the Ava-5-pilocarpine loaded was not statistically different in comparison to the negative control (HDPE). On the contrary, viable cell in contact with pilocarpine, pilocarpine-loaded Ava-1 and pilocarpine-loaded Ava-2 were significantly more numerous than the ones in contact both with HDPE and pilocarpine; the number of cells in contact with the hydrogel reached the highest value for pilocarpine-loaded Ava-2, decreased for pilocarpine-loaded Ava-1 and reached the lowest value for the pilocarpine-loaded Ava-5. This trend may be due to the different cross-linking degree of the hydrogels. In fact, the Ava-2, with an intermediate cross-linking degree, showed a structure which promotes an optimal drug release. The effect of pilocarpine released from the Ava-2 sample was evaluated at intervals of 24 hrs for a total incubation time of 96 hrs. Every 24 hrs the samples were removed and placed on new cell layer in the presence of fresh medium. The results showed that the released pilocarpine led to increase the percentage of viable cells from 0 to 24 h, from 24 to 48 h and from 48 to 72 h. The maximum cell viability was obtained with the drug released from 24 to 48 h. From 72 to 96 h the amount of released drug was not able to significantly influence the cell viability, which resulted to be the same of both HDPE and native Ava-2. This is in line with the above reported results on the release of pilocarpine from the gel Ava-2 at 36°C (Figure 10).

Conclusion

The study of polymeric systems bearing ionic or ionizable groups is always of current interest in many fields of application, expecially in the biomedical one [1,4,5]. Multiple stimuli-responsive hydrogels offer

the greatest promise of emulating biological systems due to their hydrophilic nature and tunable responses to physiologically relevant stimuli such as pH, temperature, ionic strength, and reductive environments [13]. Additionally, remote-control systems such as alternating magnetic fields, may be used to trigger a response in the material [113-115]. The purposely designed hydrogels, containing α-aminoacid residues and showing a good biocompatibility, have demonstrated to be promising candidates as soft materials [5,24]. They can provide suitable vehicles for the controlled release of drugs under determined conditions. The electrostatic interaction of a drug with a hydrogel may constitute a strategy of administering the drug through a sustained-release for a long period and preserving it from degradation phenomena [12,41,44,45,52]. In addition, the control of drug release may avoid the side effects associated with a massive administration of therapies, usual in clinical practice. The hydrogels bearing residues of L-phenylalanine or L-valine are well suited to design a delivery system of the drug containing basic functionalities in its molecule. The ionized form of the drug may interact with the anionic gel giving rise to complex systems drug-polymer of suitable stability. High values of the basicity constants (logK) generally provide a greater stability of the adduct. Consequently, this is reflected in a slower release process of the drug when the system is in contact with biological fluids. The potential application of hydrogels as a platform for drug delivery in cancer, glaucoma and depression treatment have been explored and addressed in this issue to improve their efficacy to restore a high quality of life for patients. Progress of these challenges would greatly expand the potential of hydrogel-based drug release, to successfully deliver the drug at the desired rate and location in the body [35-40].

References

1. Chaterji S, Kwon IK, Park K (2007) Smart Polymeric Gels: Redefining the Limits of Biomedical Devices. Prog Polym Sci 32: 1083-1122.
2. Qiu Y, Park K (2001) Environment-sensitive hydrogels for drug delivery. Adv Drug Deliv Rev 53: 321-339.
3. Lee SC, Kwon IK, Park K (2013) Hydrogels for delivery of bioactive agents: a historical perspective. Adv Drug Deliv Rev 65: 17-20.
4. Hoare TR, Kohane DS. Hydrogels in drug delivery: progress and challenges. Polymer 2008; 49: 1993-2007.
5. Casolaro M, Casolaro I (2013) Multiple stimuli-responsive hydrogels based on α-aminoacid residues for drug delivery. In: Alvarez-Lorenzo C, Concheiro A, editors. Smart materials for drug delivery. RSC Publ., Cambridge, UK, pp: 199-227.
6. Ahmed EM (2015) Hydrogel: Preparation, characterization, and applications: A review. J Adv Res 6: 105-121.
7. Demadis DK, Bruckner SI, Brunner E, Paasch S (2015) The intimate role of imidazole in the stabilization of silicic acid by a pH-responsive, histidine-grafted polyampholyte. Chem Mat 27: 6827-6836.
8. Du X, Zhou J, Shi J, Xu B (2015) Supramolecular Hydrogelators and Hydrogels: From Soft Matter to Molecular Biomaterials. Chem Rev 115: 13165-13307.
9. Peppas NA, Hilt JZ, Khademhosseini A (2006) Hydrogels in biology and medicine: from molecular principles to bionanotechnology. Adv Mater 18: 1345-1360.
10. Kopecek J (2007) Hydrogel biomaterials: a smart future. Biomaterials 28: 5185-5192.
11. Hoffman AS (2012) Hydrogels for biomedical applications. Adv Drug Deliv Rev 64:18-23.
12. Casolaro M, Cini R, Del Bello B, Ferrali M, Maellaro E (2009) Cisplatin/hydrogel complex in cancer therapy. Biomacromolecules 10: 944-949.
13. Knipe JM, Peppas NA (2014) Multi-responsive hydrogels for drug delivery and tissue engineering applications. Regen Biomater 1: 57-65.
14. Casolaro M (1996) Stimuli-responsive polymers. In: Salamone JC, editor. Polymeric Materials Encyclopedia. CRC Press, Boca Raton, NY, pp: 7979-7992.
15. Casolaro M, Bottari S, Ito Y (2006) Vinyl polymers based on L-histidine residues. Part 2. Swelling and electric behaviour of smart poly(ampholyte) hydrogels for biomedical applications. Biomacromolecules 7: 1439-1448.
16. Tanaka T, Nishio I, Sun ST, Ueno-Nishio S (1982) Collapse of gels in an electric field. Science 218: 467-469.
17. Murdan S (2003) Electro-responsive drug delivery from hydrogels. J Control Release 92: 1-17.
18. Janmey PA, Slochower DR, Wang YH, Wen Q, Cabers A (2014) Polyelectrolyte properties of filamentous biopolymers and their consequences in biological fluids. Soft Matter 10: 1439-1449.
19. Li W, Zhao P, Lin C (2013) Natural polyelectrolyte self-assembled multilayers based on collagen and alginate: stability and cytocompatibility. Biomacromolecules 14: 2647-2656.
20. Doillon CJ, Dunn MG, Bender E, Silver FH (1985) Collagen fiber formation in repair tissue: development of strength and toughness. Coll Relat Res 5: 481-492.
21. Bae YH, Okano T, Kim SW (1990) Temperature dependence of swelling of cross-linked poly (N,N'-alkyl substituted acrylamide) in water. J Polym Sci Polym Phys 28: 923-936.
22. Feil H, Bae YH, Feijen J (1993) Effect of copolymer hydrophilicity and ionization on the lower critical solution temperature of N-isopropylacrilamide copolymers. Macromolecules 26: 2496-2500.
23. Schmaljohann D (2006) Thermo and pH-responsive polymers in drug delivery. Adv Drug Deliv Rev 58: 1655-1670.
24. Casolaro M, Casolaro I (2012) Multiple stimuli-responsive hydrogels for metal-based drug therapy. Polymers 4: 964-985.
25. Casolaro M, Ito Y, Ishii T (2008) Stimuli-responsive poly(ampholyte)s containing L-histidine residues: synthesis and protonation thermodynamics of methacrylic polymers in the free and in the cross-linked gel forms. eXPRESS Polym. Lett 2: 165-183.
26. Heskins M, Guillet E (1968) Solution properties of poly(N-isopropylacrylamide). J Macromol Sci Chem A2: 1441-1455.
27. Hoffman AS (2014) Poly(NIPAAm) revisited-it has been 28 years since it was first proposed for use as a biomaterial: Original research article: Applications of thermally reversible polymers hydrogels in therapeutics and diagnostics, 1987; thermally reversible hydrogels: II. Delivery and selective removal of substances from aqueous solutions, 1986; a novel approach for preparation of pH-sensitive hydrogels for enteric drug delivery, 1991. J Control Release 190: 36-40.
28. Schild HG, Tirrel DA (1990) Microcalorimetric detection of lower critical solution temperature in aqueous polymer solutions. J Phys Chem 94: 4352-4356.
29. Iwata H, Oodate H, Uyama Y (1991) Preparation of temperature-sensitive membranes by graft-polymerization onto a porous membrane. J Membr Sci 55: 119-130.
30. Casolaro M, Barbucci R (1996) Thermodynamic behaviour of polyelectrolytes with the lower critical solution temperature (LCST) phenomenon. Polym Adv Techn 7: 831-838.
31. Lee KY, Mooney DJ (2001) Hydrogels for tissue engineering. Chem Rev 101: 1869-1879.
32. Van der Linden HJ, Herber S, Olthuis W, Bergveld P (2003) Stimulus-sensitive hydrogels and their applications in chemical (micro)analysis. Analyst 128: 325-331.
33. Wang KL, Burban JH, Cussler EL (1993) Hydrogels as separation agents. Adv Polym Sci 110: 67-79.
34. Bennett SL, Melanson DA, Torchiana DF, Wiseman DM, Sawhney AS (2003) Next-generation hydrogel films as tissue sealants and adhesion barriers. J Card Surg 18: 494-499.
35. Kretlow JD, Klouda L, Mikos AG (2007) Injectable matrices and scaffolds for drug delivery in tissue engineering. Adv Drug Deliv Rev 59: 263-273.

36. Worthington P, Pochan DJ, Langhans SA (2015) Peptide Hydrogels-Versatile Matrices for 3D Cell Culture in Cancer Medicine. Front Oncol 5: 92.
37. McMurtrey RJ (2014) Patterned and functionalized nanofiber scaffolds in 3-dimensional hydrogel constructs enhance neurite outgrowth and directional control. J Neural Engineering 11: 1-19.
38. El-Sherbiny IM, Yacoub MH (2013) Hydrogel scaffolds for tissue engineering: Progress and challenges. Glob Cardiol Sci Pract 316-342.
39. Tallawi M, Rosellini E, Barbani N, Cascone MG, Rai R, et al. (2015) Strategies for the chemical and biological functionalization of scaffolds for cardiac tissue engineering: a review. J R Soc Interface 12: 20150254.
40. Garg T, Singh O, Arora S, Murthy R (2012) Scaffold: a novel carrier for cell and drug delivery. Crit Rev Ther Drug Carrier Syst 29: 1-63.
41. Casolaro M, Del Bello B, Maellaro E (2011) Hydrogel containing L-valine residues as a platform for cisplatin chemotherapy. Colloids Surf B Biointerfaces 88: 389-395.
42. Tamasi G, Serinelli F, Consumi M (2008) Release studies from smart hydrogels as carriers for piroxicam and copper(II)-oxicam complexes as anti-inflammatory and anti-cancer drugs. X-ray structures of new copper(II)-piroxicam and isoxicam complex molecules. J Inorg Biochem 102: 1862-1873.
43. Tamasi G, Casolaro M, Magnani A (2010) New platinum-oxicam complexes as anti-cancer drugs. Synthesis, characterization, release studies from smart hydrogels, evaluation of reactivity with selected proteins and cytotoxic activity *in vitro*. J Inorg Biochem 104: 799-814.
44. Casolaro M, Casolaro I, Lamponi S (2012) Stimuli-responsive hydrogels for controlled pilocarpine ocular delivery. Eur J Pharm Biopharm 80: 553-561.
45. Casolaro M, Casolaro I (2015) Controlled release of antidepressant drugs by multiple stimuli-sensitive hydrogels based on α-aminoacid residues. J Drug Deliv Sci Techn 30: 82-89.
46. Casolaro M (1994) Thermodynamics of multiple stimuli-responsive polyelectrolytes with complexing ability towards the copper (II) ion. React Polym 23: 71-83.
47. Iwakura Y, Toda F, Suzuki H (1967) Synthesis of N-[1-(substituted 2 oxopropyl)]acrylamides and-methacrylamides. Isolation and some reactions of intermediates in the Dakin-West reaction. J Org Chem 32: 440-443.
48. Tamasi G, Casolaro M, Cini R (2012) X-ray structure and computational study for N-acryloyl-L-valine, a versatile monomer for preparing smart drug delivery carriers. J Molec Struct 1029: 98-105.
49. Casolaro M, Paccagnini E, Mendichi R (2005) Stimuli-responsive polymers based on L-phenylalanine residues: protonation thermodynamics of free polymers and cross-linked hydrogels. Macromolecules 38: 2460-2468.
50. Casolaro M (1998) Intelligent polymer systems for molecular separation and controlled delivery of drugs. In: Ottenbrite R, editor. Frontiers in biomedical polymer applications. Technomic Publ. Co. Inc., Lancaster, pp: 109-122.
51. Gavira JA, Cera-Manjarres A, Ortiz K, Mendez J, Jimenez-Torres JA, et al. (2014) Use of Cross-Linked Poly(ethylene glycol)-Based Hydrogels for Protein Crystallization. Cryst Growth Des 14: 3239-3248.
52. Casolaro M, Casolaro I, Bottari S, Del Bello B, Maellaro E, et al. (2014) Long-term doxorubicin release from multiple stimuli-responsive hydrogels based on α-amino acid residues. Eur J Pharm Biopharm 88: 424-433.
53. Barbucci R, Pasqui D, Giani G (2011) A novel strategy for engineering hydrogels with ferromagnetic nanoparticles as crosslinkers of the polymer chains. Potential applications as a targeted drug delivery system. Soft Matter 7: 5558-5565.
54. Lu AH, Salabas EL, Schüth F (2007) Magnetic nanoparticles: synthesis, protection, functionalization and application. Angew Chem Int Ed Engl 46: 1222-1244.
55. Hernandez R, Sacristan J, Nogales A (2009) Structural organization of iron oxide nanoparticles synthesized inside hybrid polymer gels derived from alginate studied with small-angle X-ray scattering. Langmuir 25: 13212-13218.
56. Albert A (1968) Selective Toxicity London: Methuen.
57. Nishiyama N, Suzuki K, Nagatsuka A (2003) Dissociation states of collagen functional groups and their effects on the priming efficacy of HEMA bonded to collagen. J Dent Res 82: 257-261.
58. Dobrynin AV, Rubinstein M (2005) Theory of polyelectrolytes in solutions and at surfaces. Prog Polym Sci 30: 1049-1118.
59. Barbucci R, Casolaro M, Magnani A (1992) Ionic and ionizable synthetic polymers: interactions in aqueous solution. Coord Chem Rev 120: 29-50.
60. Casolaro M (1997) Solution behaviour of poly (N-acryloyl-L-leucine) and its copolymers with N- isopropylacrylamide. Polymer 38: 4215-4222.
61. Casolaro M (1995) Vinyl polymers containing L-valine and L-leucine residues: thermodynamic behaviour of homopolymers and copolymers with N-isopropylacrylamide. Macromolecules 28: 2351-2358.
62. Casolaro M, Bottari S, Cappelli A, Mendichi R, Ito Y (2004) Vinyl polymers based on L-histidine residues. Part 1. The thermodynamics of poly(ampholyte)s in the free and in the cross-linked gel form. Biomacromolecules 5: 1325-1332.
63. Wada A, Ishii T, Casolaro M (2007) Copolymers including L-histidine and hydrophobic moiety for preparation of nonbiofouling surface. Biomacromolecules 8: 3340-3344.
64. Casolaro M, Chelli M, Ginanneschi M, Laschi F, Messori L, et al. (2002) Spectroscopic and potentiometric study of the SOD mimic system copper(II)/acetyl-L-histidylglycyl-L-histidylglycine. J Inorg Biochem 89: 181-190.
65. Barbucci R, Casolaro M, Danzo N (1983) Effect of different shielding groups on the polyelectrolyte behaviour of poly(amine)s. Macromolecules 16: 456-462.
66. Katchalsky A, Spitnik P (1947) Potentiometric titrations of polymethacrylic acid. J Polym Sci 2: 432-446.
67. Ficocelli S (2014) La depressione oscura il nostro futuro. La Repubblica.it, October 17th.
68. Substance Abuse and Mental Health Services Administration (2014) Results from the 2013 National Survey on Drug Use and Health: Mental Health Findings. Rockville: MD.
69. Marcus SM, Kerber KB, Rush AJ (2008) Sex differences in depression symptoms in treatment-seeking adults: confirmatory analyses from the Sequenced Treatment Alternatives to Relieve Depression study. Compr. Psychiatry 49: 238-246.
70. [No authors listed] (2010) Extended-release trazodone (Oleptro) for depression. Med Lett Drugs Ther 52: 91-92.
71. Bossini L, Casolaro I, Koukouna D, Cecchini F, Fagiolini A (2012) Off-label uses of trazodone: a review. Expert Opin Pharmacother 13: 1707-1717.
72. Bossini L, Coluccia A, Casolaro I, Benbow J, Amodeo G, et al. (2015) Off-Label Trazodone Prescription: Evidence, Benefits and Risks. Curr Pharm Des 21: 3343-3351.
73. Fagiolini A, Comandini A, Catena Dell'Osso M, Kasper S (2012) Rediscovering trazodone for the treatment of major depressive disorder. CNS Drugs 26: 1033-1049.
74. Abdouss M, Asadi E, Azodi-Deilami S, Beik-mohammadi N, Aslanzadeh SA (2011) Development and characterization of molecularly imprinted polymers for controlled release of citalopram. J Mater Sci Mater Med 22: 2273-2281.
75. Das MK, Bhattacharya A, Ghosal SK (2006) Transdermal delivery of trazodone hydrochloride from acrylic films prepared from aqueous latex. Indian J Pharm Sci 68: 41-46.
76. Murray CJ, Lopez AD (1997) Alternative projections of mortality and disability by cause 1990-2020: Global Burden of Disease Study. Lancet 349: 1498-1504.
77. Bezchlibnyk Butler K, Aleksic I, Kennedy SH (2000) Citalopram: a review of pharmacological and clinical effects. J Psychiatry Neurosci 25: 241-254.
78. Burghardt NS, Sullivan GM, McEwen BS (2004) The selective serotonin reuptake inhibitor citalopram increases fear after acute treatment but

reduces fear with chronic treatment: a comparison with tianeptine. Biol Psychiatry 55: 1171-1178.

79. Ishak WW, Christensen S, Sayer G, Ha K, Li N, et al. (2013) Sexual satisfaction and quality of life in major depressive disorder before and after treatment with citalopram in the STAR*D study. J Clin Psychiatry 74: 256-261.
80. Mansari ME, Wiborg O, Mnie-Filali O, Benturquia N, Sánchez C, et al. (2007) Allosteric modulation of the effect of escitalopram, paroxetine and fluoxetine: in-vitro and in-vivo studies. Int J Neuropsychopharmacol 10: 31-40.
81. Morishita S, Arita S (2003) Induction of mania in depression by paroxetine. Hum Psychopharmacol 18: 565-568.
82. Ruiz R, Ràfols C, Rosés M (2003) A potentially simpler approach to measure aqueous pKa of insoluble basic drugs containing amino groups. J Pharm Sci 92: 1473-1481.
83. Shalaeva M, Kenseth J, Lombardo F (2008) Measurement of dissociation constants (pKa values) of organic compounds by multiplexed capillary electrophoresis using aqueous and cosolvent buffers. J Pharm Sci 97: 2581-2606.
84. Cini R, Defazio S, Tamasi G (2007) fac-{Ru(CO)3}2+-core complexes and design of metal-based drugs. Synthesis, structure, and reactivity of Ru-thiazole derivative with serum proteins and absorption-release studies with acryloyl and silica hydrogels as carriers in physiological media. Inorg Chem 46:79-92.
85. Tamasi G, Bernini C, Corbini G, Owens NF, Messori L, et al. (2014) Synthesis, spectroscopic and DFT structural characterization of two novel ruthenium(III) oxicam complexes. In vivo evaluation of anti-inflammatory and gastric damaging activities. J Inorg Biochem 134: 25-35.
86. Lippert B (1999) Cisplatin Wiley-VCH: Weinheim
87. DeConti RC, Toftness BR, Lange RC, Creasey WA (1973) Clinical and pharmacological studies with cis-diamminedichloroplatinum (II). Cancer Res 33: 1310-1315.
88. Andronescu E, Ficai A, Albu MG, Mitran V, Sonmez M, et al. (2013) Collagen-hydroxyapatite/cisplatin drug delivery systems for locoregional treatment of bone cancer. Technol Cancer Res Treat 12: 275-284.
89. Yan X, Gemeinhart A (2005) Cisplatin delivery from poly(acrylic acid-co-methyl methacrylate) microparticles. J Controlled Rel 106: 198-208.
90. Park H, Robinson JR (1987) Mechanisms of mucoadhesion of poly(acrylic acid) hydrogels. Pharm Res 4: 457-464.
91. Bignotti F, Casolaro M, D'Amore A (2001) Stimuli-responsive polymers based on N- isopropylacrylamide and N-methacryloyl-L-leucine. Macromol Chem Phys 202: 1150-1155.
92. Bignotti F, Casolaro M, D'Amore A (2000) Synthesis, characterization and solution behaviour of intelligent polymers bearing L-leucine residues in the side chains. Polymer 41: 8247-8256.
93. Ali M, Horikawa S, Venkatesh S (2007) Zero-order therapeutic release from imprinted hydrogel contact lenses within in-vitro physiological ocular tear flow. J Controlled Rel 124: 154-162.
94. Kim JH, Lee SB, Kim SJ, (2002) Rapid temperature/pH response of porous alginate-g-poly(N-isopropylacrylamide) hydrogels. Polymer 43: 7549-7558.
95. Brazel CS, Peppas NA (2000) Modeling of drug release from swellable polymers. Eur J Pharm Biopharm 49: 47-58.
96. Ballou LM, Lin RZ (2008) Rapamycin and mTOR kinase inhibitors. J Chem Biol 1: 27-36.
97. Jhunjhunwala S, Raimondi G, Thomson AW, Little SR (2009) Delivery of rapamycin to dendritic cells using degradable microparticles. J Control Release 133: 191-197.
98. Fisher SJ, Benson LM, Fauq A (2008) Cisplatin and dimethyl sulfoxide react to form an adducted compound with reduced cytotoxicity and neurotoxicity. Neurotoxicology 29: 444-452.
99. Sundquist WI, Ahmed KJ, Hollis LS (1987) Solvolysis reactions of cis- and trans-diamminedichloroplatinum(II) in dimethyl sulfoxide. Structural characterization and DNA bonding of trans-bis(amine)chloro(DMSO)platinum(1+). Inorg Chem 26: 1524-1528.
100. Thallinger C, Poeppl W, Pratscher B, Mayerhofer M, Valent P, et al. (2007) CCI-779 plus cisplatin is highly effective against human melanoma in a SCID mouse xenotranplantation model. Pharmacology 79: 207-213.
101. Frederick CA, Williams LD, Ughetto G, van der Marel GA, van Boom JH, et al. (1990) Structural comparison of anticancer drug-DNA complexes: adriamycin and daunomycin. Biochemistry 29: 2538-2549.
102. Dadsetan M, Liu Z, Pumberger M, Giraldo CV, Ruesink T, et al. (2010) A stimuli-responsive hydrogel for doxorubicin delivery. Biomaterials 31: 8051-8062.
103. Subedi RK, Kang KW, Choi HK (2009) Preparation and characterization of solid lipid nanoparticles loaded with doxorubicin. Eur J Pharm Sci 37: 508-513.
104. Chouhan R, Bajpai A (2009) Real time *in vitro* studies of doxorubicin release from PHEMA nanoparticles. J Nanobiotechnology 7: 5.
105. Ghugare SV, Mozetic P, Paradossi G (2009) Temperature-sensitive poly(vinyl alcohol)/poly(methacrylate-co-N-isopropylacrylamide) microgels for doxorubicin delivery. Biomacromolecules 10: 1589-1596.
106. Lavignac N, Nicholls JL, Ferruti P, Duncan R (2009) Poly(amidoamine) conjugates containing doxorubicin bound via an acid-sensitive linker. Macromol Biosci 9: 480-487.
107. Loh XJ, del Barrio J, Toh PPC (2011) Triply triggered doxorubicin release from supramolecular nanocontainers. Biomacromolecules 13: 84-91.
108. Meenach SA, Shapiro JM, Hilt JZ, Anderson KW (2013) Characterization of PEG-iron oxide hydrogel nanocomposites for dual hyperthermia and paclitaxel delivery. J Biomater Sci Polym Ed 24: 1112-1126.
109. Needham D, Dewhirst MW (2013) Materials science and engineering of low temperature sensitive liposome (LTSL): composition-structure-property relationship that underlie its design and performance. In: Alvarez-Lorenzo C, Concheiro A, editors. Smart materials for drug delivery. RSC Publ.: Cambridge, UK, pp: 33-79.
110. Gerweck LE, Vijayappa S, Kozin S (2006) Tumor pH controls the in vivo efficacy of weak acid and base chemotherapeutics. Mol Cancer Ther 5: 1275-1279.
111. Sanson C, Schatz C, Le Meins JF, Soum A, Thévenot J, et al. (2010) A simple method to achieve high doxorubicin loading in biodegradable polymersomes. J Control Release 147: 428-435.
112. Satarkar NS, Hilt JZ (2008) Magnetic hydrogel nanocomposites for remote controlled pulsatile drug release. J Control Release 130: 246-251.
113. Marques C, Ferreira JM, Andronescu E, Ficai D, Sonmez M, et al. (2014) Multifunctional materials for bone cancer treatment. Int J Nanomedicine 9: 2713-2725.
114. Hu K, Sun J, Guo Z (2015) A novel magnetic hydrogel with aligned magnetic colloidal assemblies showing controllable enhancement of magnetothermal effect in the presence of alternating magnetic field. Adv Mat 27: 2507-2514.
115. Thoniyot P, Tan MJ, Karim AA (2015) Nanoparticle-hydrogel composites: concept, design, and applications of these promising, multi-functional materials. Adv Sci 2: 1-13.
116. Ortner V, Kaspar C, Halter C, Töllner L, Mykhaylyk O, et al. (2012) Magnetic field-controlled gene expression in encapsulated cells. J Control Release 158: 424-432.
117. Barbucci R, Giani G, Fedi S (2012) Biohydrogels with magnetic nanoparticles as crosslinker: characteristics and potential use for controlled antitumor drug-delivery. Acta Biomater 8: 4244-4252.
118. Lu Z, Prouty MD, Guo Z, Golub VO, Kumar CS, et al. (2005) Magnetic switch of permeability for polyelectrolyte microcapsules embedded with Co@Au nanoparticles. Langmuir 21: 2042-2050.
119. Hu SH, Liu TY, Huang HY, Liu DM, Chen SY (2008) Magnetic-sensitive silica nanospheres for controlled drug release. Langmuir 24: 239-244.
120. Liu J, Zhang Y, Wang C (2010) Magnetically sensitive alginate-templated polyelectrolyte multilayer microcapsules for controlled release of doxorubicin. J Phys Chem C 114: 7673-7679.

121. Peppas NA, Korsmeyer RW (1987) Dynamically swelling hydrogels in controlled release applications. In: Peppas NA, editor. Hydrogels in medicine and pharmacy. CRC Press: Boca Raton, FL, pp: 109-136.
122. Peppas NA (2014) 1. Commentary on an exponential model for the analysis of drug delivery: Original research article: a simple equation for description of solute release: I II. Fickian and non-Fickian release from non-swellable devices in the form of slabs, spheres, cylinders or discs, 1987. J Control Release 190: 31-32.
123. Missirlis D, Kawamura R, Tirelli N, Hubbell JA (2006) Doxorubicin encapsulation and diffusional release from stable, polymeric, hydrogel nanoparticles. Eur J Pharm Sci 29: 120-129.
124. Bardajee YGR, Hooshyas Z, Asli MJ (2014) Synthesis of a novel supermagnetic iron oxide nanocomposite hydrogel based on graft copolymerization of poly((2 dimethylamino)ethyl-methacrylate) onto salep for controlled release of drug. Mater Sci Eng C 36: 277-286.
125. Bartlett JD, Jaanus SD (2008) Clinical Ocular Pharmacology. Elsevier Health Sciences.
126. Meloun M, Cernohorský P (2000) Thermodynamic dissociation constants of isocaine, physostigmine and pilocarpine by regression analysis of potentiometric data. Talanta 52: 931-945.
127. Lee P, Shen Y, Eberle M (1975) The long-acting Ocusert-pilocarpine system in the management of glaucoma. Invest Ophthalmol 14: 43-46.
128. Ludwig A (2005) The use of mucoadhesive polymers in ocular drug delivery. Adv Drug Deliv Rev 57: 1595-1639.
129. Verestiuc L, Ivanov C, Barbu J (2004) Dual-stimuli-responsive hydrogels based on poly(N-isopropylacrylamide)/chitosan semi-interpenetrating networks. Int J Pharm 269: 185-194.
130. Gupta SK, Agarwal R, Galpalli ND, Srivastava S, Agrawal SS, et al. (2007) Comparative efficacy of pilocarpine, timolol and latanoprost in experimental models of glaucoma. Methods Find Exp Clin Pharmacol 29: 665-671.
131. Rathore KS, Nema RK (2009) Review on ocular inserts. Int J Pharm Tech Res 1: 164-169.
132. Anumolu SS, Singh Y, Gao D, Stein S, Sinko PJ (2009) Design and evaluation of novel fast forming pilocarpine-loaded ocular hydrogels for sustained pharmacological response. J Control Release 137: 152-159.
133. Hsiue GG, Guu JA, Cheng CC (2001) Poly(2-hydroxyethyl methacrylate) film as a drug delivery system for pilocarpine. Biomaterials 22: 1763-1769.
134. Perrin DD (1995) Dissociation constants of organic bases in aqueous solution. Butterworths: London.
135. Yoshida R, Sakai K, Okano T (1994) Modulating the phase transition temperature and thermosensitivity in N-isopropylacrylamide copolymer gels. J Biomater Sci Polym Edn 6: 585-598.
136. Sershen SR, Westcott SL, Halas NJ (2002) Independent optically addressable nanoparticle-polymer optomechanical composites. Appl Phys Lett 80: 4609-4611.